International Journal of Earth Sciences (2019) 108:2627–2651
https://doi.org/10.1007/s00531-019-01780-0

ORIGINAL PAPER

# Three-dimensional geological modeling supports a revised Burdigalian chronostratigraphy in the North Alpine Foreland Basin

**Felix Hofmayer[1,2] · Uwe Kirscher[3] · Karin Sant[4] · Wout Krijgsman[4] · Thomas Fritzer[5] · Dietmar Jung[6] · Vinzenz Weissbrodt[7] · Bettina Reichenbacher[1]**

Received: 5 April 2019 / Accepted: 12 October 2019 / Published online: 11 November 2019


## Abstract

Precise age data are a basic prerequisite for the correlation of a sedimentary succession with the Global Time Scale, which in turn allows one to place its biotic and other data in a global context. In the North Alpine Foreland Basin (NAFB), a patchy distribution of outcrops and uncertainties in the correlation of strata have led to conflicting age models, in particular for deposits of lower Miocene (Burdigalian) age. Here, we present a new three-dimensional geological model of the SE German sector of the NAFB, covering an area of 13,200 km$^2$, which helps to resolve the discrepancies. The dataset comprises lithostratigraphic information from 150 boreholes, supplemented by magnetostratigraphic data from six outcrops. Computer-based 3D modeling was conducted with the open source software QGIS for a 500-m-thick succession comprising units of the Upper Marine Molasse, the brackish Oncophora Fm and the Upper Freshwater Molasse. The results provide new insights pertaining to (1) the isochrony of strata, (2) subsidence, and (3) synsedimentary tectonics. The new data permit us to reliably place the outcrops within the regional lithostratigraphic scheme, thus enabling a new correlation of their magnetic polarities with the Global Time Scale. On this basis, we propose a revised age model for the middle and upper Burdigalian strata in the eastern part of the NAFB, which is supported by previously reported $^{87}Sr/^{86}Sr$ age data. The model indicates that the succession is substantially—up to 0.8 Ma—younger than earlier publications have suggested. Furthermore, it implies that the two synsedimentary tectonic events discerned may both be related to the large-scale tectonic movements that affected the NAFB during the late Burdigalian.

**Keywords** S-German Molasse Basin · Ottnangian–Karpatian · 3D model · Stratigraphy · Tectonics · Sr-isotope ages

## Introduction

The North Alpine Foreland Basin (NAFB) of Central Europe is an important archive for the Oligocene–Miocene time span, because thick and often fossiliferous sedimentary successions accumulated during this interval, which provide invaluable insights into the geological evolution of

**Electronic supplementary material** The online version of this article (https://doi.org/10.1007/s00531-019-01780-0) contains supplementary material, which is available to authorized users.

✉ Bettina Reichenbacher
b.reichenbacher@lrz.uni-muenchen.de

[1] Department of Earth- and Environmental Sciences, Palaeontology and Geobiology, Ludwig-Maximilians-University, Richard-Wagner-Strasse 10, 80333 Munich, Germany

[2] Geological Survey of Austria, Neulinggasse 38, 1030 Vienna, Austria

[3] Department of Geosciences, Eberhard Karls University Tübingen, Sigwartstr. 10, 72076 Tübingen, Germany

[4] Paleomagnetic Laboratory "Fort Hoofddijk", Department of Earth Sciences, Utrecht University, Budapestlaan 17, 3584 CD Utrecht, The Netherlands

[5] Bayerisches Landesamt für Umwelt, Dienststelle Augsburg, Haunstetter Straße 112, 86161 Augsburg, Germany

[6] Bayerisches Landesamt für Umwelt, Dienststelle Hof, Hans-Högn-Straße 12, 95030 Hof/Saale, Germany

[7] Department of Earth and Environmental Sciences, Geophysics, Ludwig-Maximilians-University, Theresienstraße 41, 80333 Munich, Germany

the foreland basin and the changes in environmental conditions (Lemcke 1988; Schlunegger et al. 2001; Kuhlemann and Kempf 2002; Böhme 2003). Conversely, attempts to link the observed geological and palaeontological data to global climate change and sea-level rise or fall have been hampered, mainly because no consensus high-resolution age model for the NAFB has yet been established (see Sant et al. 2017). The reasons for the uncertainties in dating include several issues: (1) existing biostratigraphic schemes for the sediments in the NAFB, which are largely based on foraminifers, bivalves, fish otoliths, small mammals and charophytes (Cicha et al. 1998; Berger et al. 2005; Kälin and Kempf 2009), usually lack absolute age constraints based on radiometric ages; (2) many of the fossil species that are useful for regional biostratigraphy are endemic to the NAFB and/or depend on a particular facies; (3) continuous outcrops and long drill-cores are rare in the NAFB, which gives rise to uncertainties regarding correlations and isochrony of lithostratigraphic units. As a result, correlation of the biostratigraphic scheme for the NAFB with the Global Time Scale (GTS) is not straightforward and leaves room for speculation.

However, in spite of these problems, considerable progress toward a better correlation of the NAFB sediments with the GTS has been made in the last 20 years, primarily based on integrative studies combining bio-, litho- and magnetostratigraphic data, but including chemostratigraphic and other proxy data as well (e.g., Schlunegger et al. 1997; Pippèrr et al. 2007; Kälin and Kempf 2009; Grunert et al. 2015; van der Boon et al. 2018). In this context, the construction of a high-resolution age model for the sediments of the Burdigalian stage of the lower Miocene has received much attention (Kempf et al. 1999; Abdul-Aziz et al. 2010; Reichenbacher et al. 2013; Grunert et al. 2014; Pippèrr et al. 2016, 2018; Sant et al. 2017; Palzer-Khomenko et al. 2018). Despite this interest, no congruent high-resolution age model yet exists for the Burdigalian sediments in the NAFB.

The objective of this study is to test, for the first time, whether three-dimensional (3D) geological modeling can lead to an improved correlation of the Burdigalian in the NAFB with the GTS. The study area is located in the southeast German portion of the NAFB (Fig. 1a, b), covering an area of 139 × 95 km (Fig. 1c). We chose this region because it includes several outcrops from which bio- and magnetostratigraphic data can be obtained (Pippèrr et al. 2018; this

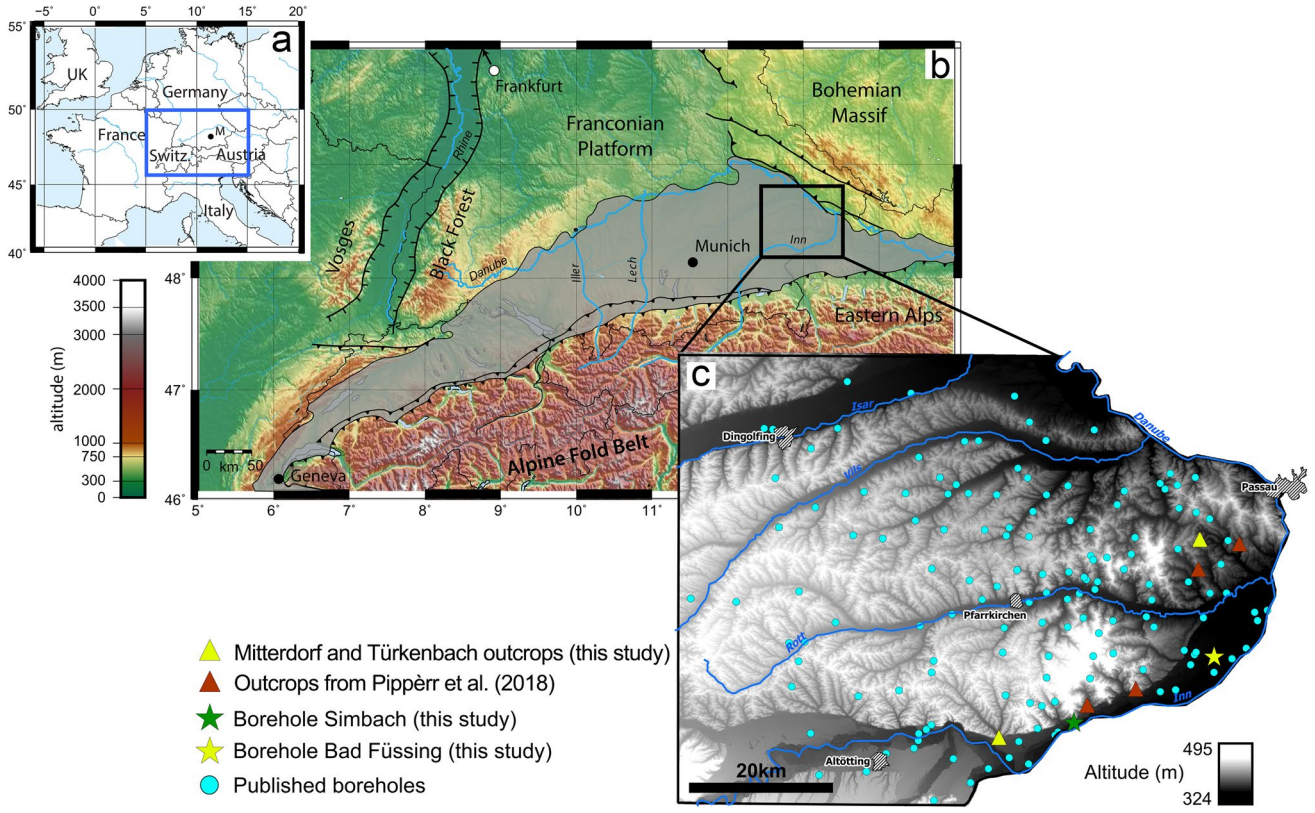


**Fig. 1** **a** Location of the North Alpine Foreland Basin (NAFB) in Europe. **b** Overview of the NAFB (or Molasse Basin) on a topographical map. The location of the study area is indicated. **c** Detailed topography of the study area (Digital Elevation Model) with locations of boreholes and outcrops; for details see Fig. 4. **a**, **b** Modified from Sant et al. (2017)

study). We postulated that 3D modeling would permit us to reliably place these outcrops within the regional lithostratigraphic scheme, thus enabling correlation of their magnetostratigraphic patterns with the GTS.

## Geological setting

### North Alpine Foreland Basin (NAFB) and Molasse Basin

The NAFB formed part of the Paratethys realm and was shaped by the Alpine Orogeny from the early Oligocene to the late Miocene (Lemcke 1988; Kuhlemann and Kempf 2002; Sissingh 2006). Its Oligo-Miocene sediments are termed *Molasse*, and the NAFB during this period is also referred to as the Molasse Basin (Fig. 1b). The Molasse Basin is asymmetrical in shape; its deepest part lies close to the Alpine thrust front and it shoals toward the north; sediments are thickest (up to 5000 m) in the south, near the Alps, and decrease toward the north, reaching only a few meters in the most distal regions (Lemcke 1988; Bachmann and Müller 1992; Doppler et al. 2005). The Molasse sediments are traditionally divided into marine, brackish and freshwater Molasse units. Two transgressive–regressive megacycles can be discriminated, with the older one extending from the lower Oligocene to the lower Miocene, and the younger spanning the lower to middle-upper Miocene. The first megacycle comprises the Lower Marine Molasse (UMM), the Lower Brackish Molasse (UBM) and the Lower Freshwater Molasse (USM), while the second megacycle encompasses the Upper Marine Molasse (OMM), the Upper Brackish Molasse (OBM) and the Upper Freshwater Molasse (see Janssen et al. 2018 and references therein).

Our work focuses on the second megacycle and its middle-to-upper Burdigalian deposits, i.e., the OMM, OBM and lowermost OSM (Fig. 2). The deposition of the OMM in the NAFB took place during the time span of the 'Burdigalian Seaway' (Allen et al. 1985; Garefalakis and Schlunegger 2019). This marine gateway connected the western Mediterranean (Rhône Basin) with the Western and Central Paratethys and led to the flooding of the NAFB from western Switzerland across south Germany into western Austria (Kuhlemann and Kempf 2002; Harzhauser and Piller 2007; Pippèrr et al. 2016). The OBM records the retreat of the sea from the NAFB and is characterized by the emergence of brackish basins; the bivalve *Rzehakia* and other endemic molluscs are typical for these deposits (Schlickum 1971; Čtyroký et al. 1973; Pippèrr and Reichenbacher 2017). Finally, a large westward-flowing river system gave rise to

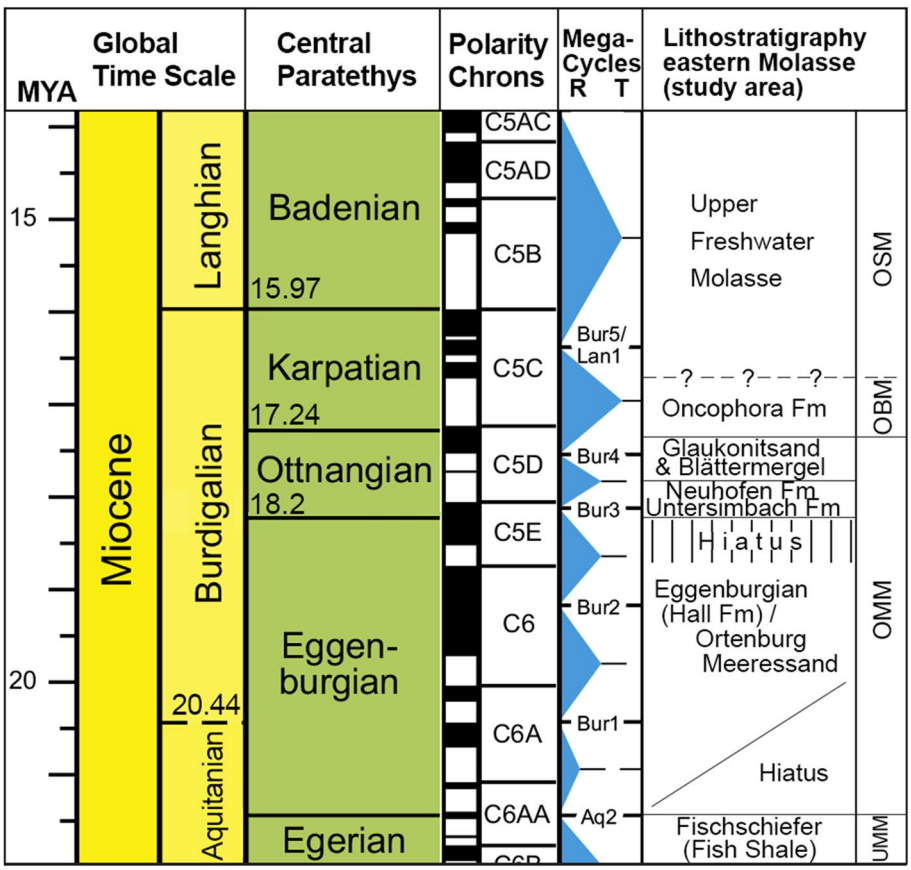


**Fig. 2** Chart depicting the Global Time Scale (GTS), Central Paratethys stratigraphy, magnetic polarities, and sequence stratigraphy according to Hilgen et al. (2012), with the base of the Ottnangian adapted from Pippèrr et al. (2018). Right columns depict the lower to middle Miocene lithostratigraphy of the eastern part of the North Alpine Foreland Basin (= eastern Molasse) and its current correlation with the GTS according to Doppler et al. (2005) and Pippèrr et al. (2018). *UMM* Lower Marine Molasse ('Untere Meeresmolasse' in German), *OMM* Upper Marine Molasse ('Obere Meeresmolasse'), *OBM* Upper Brackish Molasse ('Obere Brackwassermolasse'), *OSM* Upper Freshwater Molasse ('Obere Süßwassermolasse')

the Upper Freshwater Molasse (OSM), and remained the principal sediment supplier during the middle and late Miocene (Lemcke 1988; Prieto et al. 2009; Janssen et al. 2018).

### Study area

Our study area is located in the eastern Molasse of the south German Molasse Basin (lower Bavaria) (Fig. 1b). To the south, the area is delimited by the river Inn, which represents the border with Austria. The river Danube bounds the study area in the northeast, while the rivers Isar, Vils, Rott and Inn flow roughly eastward through the study area. District capitals are Passau, Dingolfing, Pfarrkirchen and Altötting (Fig. 1c).

Figure 2 depicts the established lithostratigraphic scheme in the study area and its current correlations with the lower Miocene Central Paratethys stages Eggenburgian, Ottnangian and Karpatian (Piller et al. 2007; Hilgen et al. 2012). The 'Ortenburg Meeressand' comprises highly fossiliferous marine sands and has been correlated with the middle Eggenburgian (Wenger 1987; Schneider 2008; Pippèrr and Reichenbacher 2009). The Untersimbach and Neuhofen formations are marine, neritic sediments and correspond to the classical lower Ottnangian of the South German and Austrian Molasse Basin (Wenger 1987; Rupp et al. 2008; Pippèrr 2011). They are overlaid by an alternation of marginal marine sands and marls, collectively named 'Glaukonitsand and Blättermergel' and traditionally referred to the middle Ottnangian; then follows the brackish Oncophora Fm, which is assigned to the upper Ottnangian-to-?lower Karpatian (see Pippèrr et al. 2018 and references therein). The Oncophora Fm is succeeded by the OSM, which generally terminates the Molasse sequence in the NAFB and is of Karpatian to Sarmatian age (Bachmann and Müller 1992; Kirscher et al. 2016; Rocholl et al. 2018).

### Tectonic structures

The general tectonic pattern in the NAFB is normal faulting with NW–SE strike (Sissingh 2006; von Hartmann et al. 2016). Figure 3a shows the tectonic structures in the eastern part of the NAFB, where NNW–SSE striking faults, especially in the northeast, contribute to the general NW–SE pattern. One possible reason for this is that, in addition to the Alps, the Bohemian Massif exerted tectonic constraints. The tectonic structures of the study region are described in detail in Lemcke (1973) and Unger and Schwarzmeier (1982) and are depicted in Fig. 3b. A prominent element is the NW–SE striking Braunau Trough. This is delimited to the southwest by the tectonic horst of the Landshut–Neuötting High. This structure, albeit not named as such, can also be recognized in Austria, where it is bounded by the Mattig fault and a further (unnamed) parallel fault (Wagner 1998). The Braunau Trough is bordered to the east by the Aidenbach–Griesbach High, which is defined by the Pocking Rupture and the Wolfach Fault (Fig. 3b). A further trough structure east of the Aidenbach–Griesbach High is the rhombus-like Ortenburg Depression, west of the city of Passau, which is delimited by the Ortenburg Rupture, the Wolfach Fault and the Kalkberg Fault (Fig. 3b). The extension of the Wolfach Fault to the south (dotted in Fig. 3b) is uncertain according to new geoelectric measurements done by the Bayerisches Landesamt für Umwelt (LfU) (pers. communication Johannes Großmann, LfU).

## Materials and methods

### Dataset

We built a stratigraphic dataset comprising both new and published information from a total of 150 boreholes and six outcrops, which served as the input for computer-based 3D modeling. The locations of all boreholes and sites considered are shown in Fig. 4. Details of all locations and stratigraphy are compiled in the Supplementary Material. Coordinates are given in the WGS 84 coordinate system (EPSG:3857). In the supplementary material coordinates are specified in the Gauss-Krüger Zone 4 coordinate system (EPSG:31468).

Stratigraphic information was obtained for each data point using available lithostratigraphic and sedimentological information (see "Methods"). All established lithostratigraphic units of the Burdigalian are included in the dataset, i.e., 'Ortenburg Meeressand' [Ortenburg Marine Sand], Untersimbach Formation (US Fm), Neuhofen Formation (NH Fm), Littoral facies of Holzbach and Höch (Li HH), 'Glaukonitsand and Blättermergel' [Glauconite Sand and Foliated Marl] (GS-BM), 'Ortenburg Schotter' [Ortenburg Gravel], Oncophora Formation (Onc Fm) and Upper Freshwater Molasse (OSM) (Fig. 2). Subunits recorded in the drilling data as 'Glaukonitsands', 'Brombacher Sande' and 'Blättermergel' were assimilated to the GS-BM. The Onc Fm consists of lower and upper Onc Fm and a total of seven horizons (Schlickum and Strauch 1968; Pippèrr et al. 2018). In the model, these subunits were all subsumed into the Onc Fm. Similarly, subunits or gravel layers within the OSM were all treated as OSM.

#### New data

**Outcrop Mitterdorf** The outcrop is an actively mined clay pit located to the north of the village of Mitterdorf (48°29′56.2″ N, 13°16′60.0″ E), about 15 km SW of Passau (Fig. 3). In the years 2014 and 2015, a succession of clayey marls of the NH Fm, about 14 m thick, was exposed at this site, which has been studied by Pippèrr et al. (2018). These authors assigned the section to the lower Ottnangian based on the

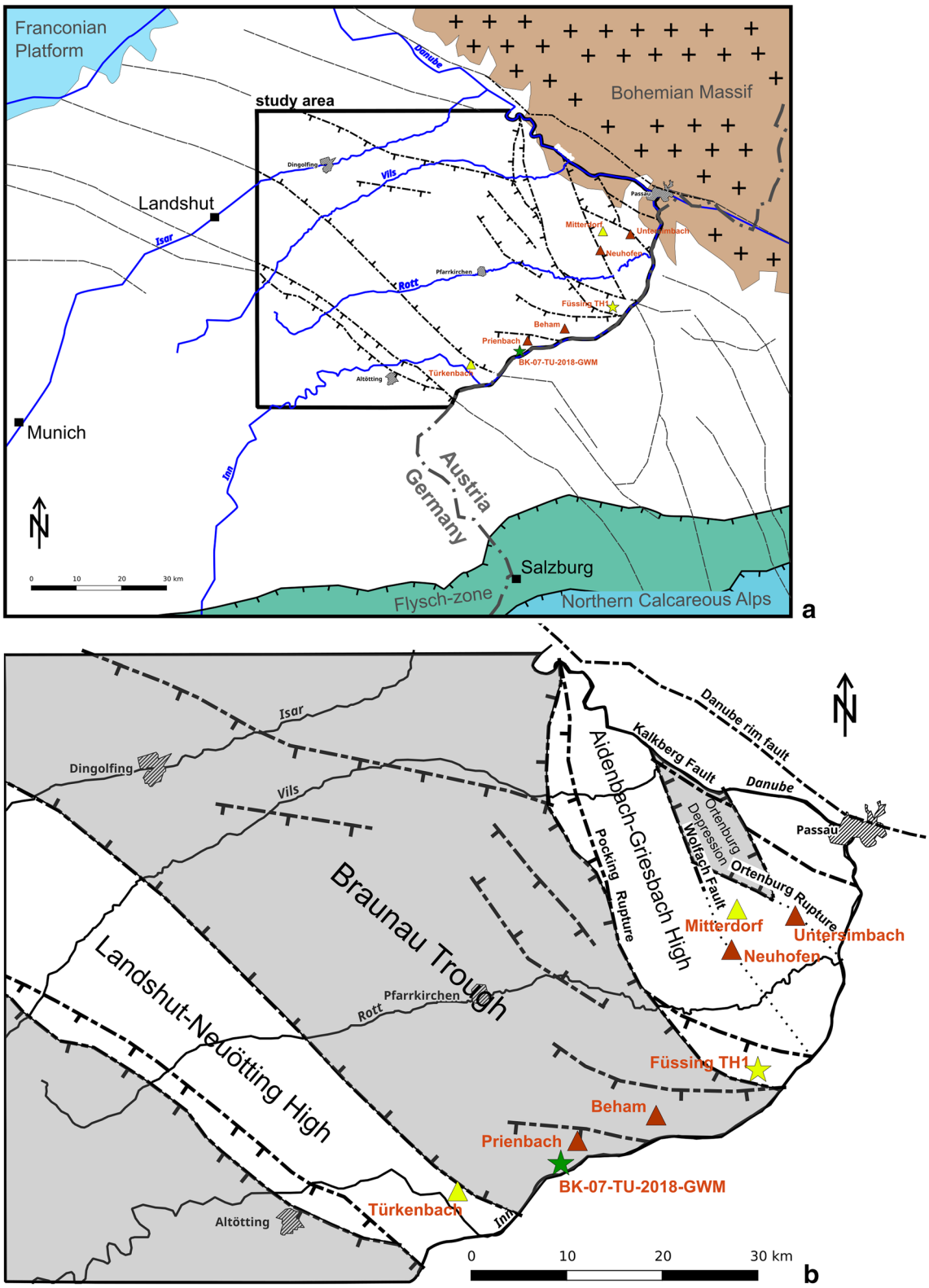


**Fig. 3** **a** Location of the study area in the eastern part of the NAFB, with tectonic structures (adapted from Lemcke 1973; Unger and Schwarzmeier 1982; Wagner 1998), and locations of outcrops and new boreholes. **b** Close-up of the study area, depicting names of faults and tectonic structures. For legend, see Fig. 1

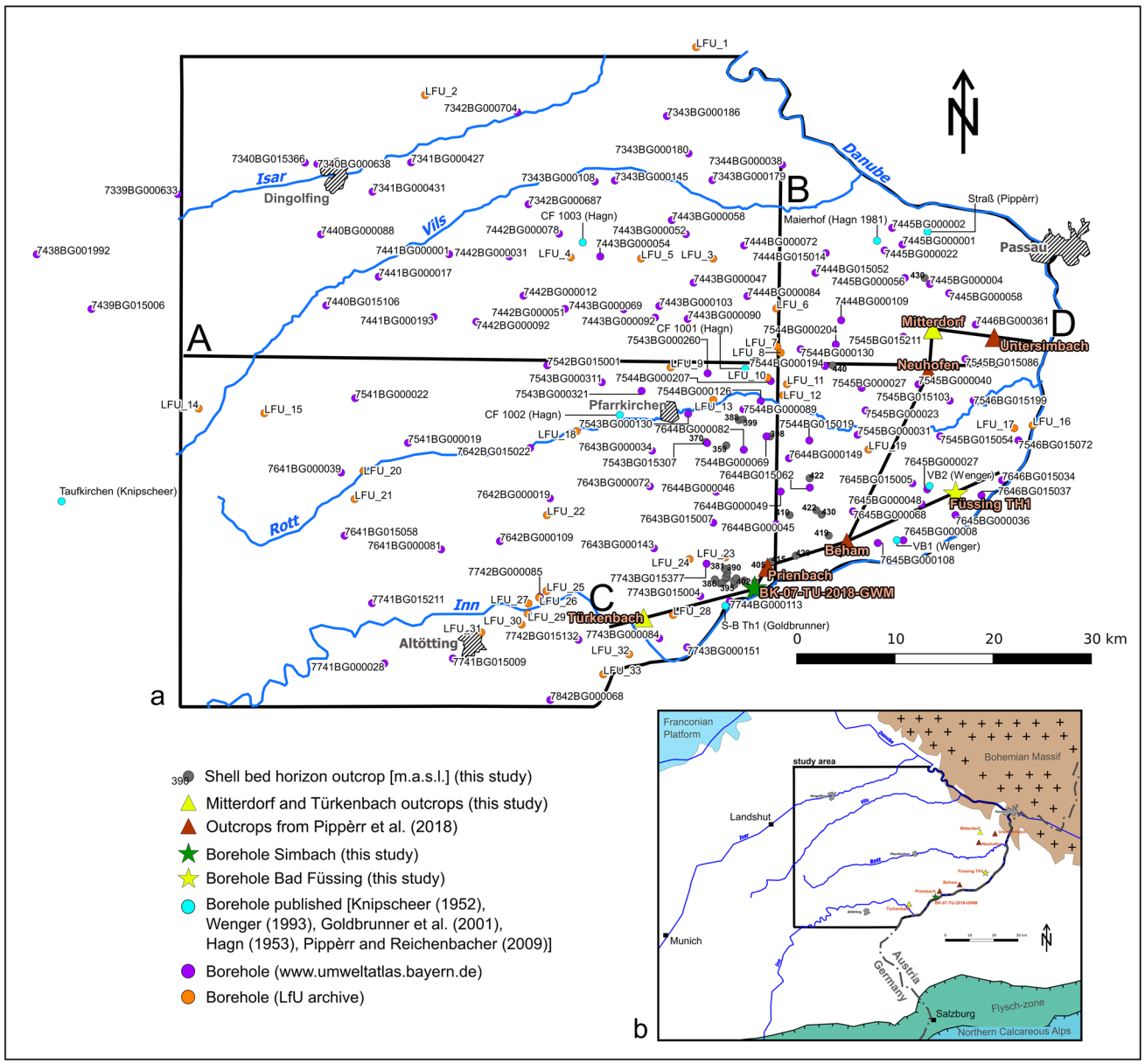


**Fig. 4** **a** Study area with locations of the boreholes and outcrops for which data were incorporated into the 3D model and sites of outcrops. Labels indicate ID number of corresponding borehole and literature source, respectively (see Supplementary Data for details). Capital letters indicate positions of the profiles shown in Figs. 9 and 10. **b** Overview of the study area in the SE German part of the NAFB

benthic foraminiferal assemblages. In addition, Pippèrr et al. (2018) detected a reverse polarity in the lower and middle part of the section and proposed its correlation with the polarity chron C5Dr2r, which dates to ~ 17.9–18.0 Ma. In the uppermost part of the clay pit, Pippèrr et al. (2018) detected a 3-m sequence with normal polarity, albeit with some uncertainty due to the sedimentological conditions (see Pippèrr et al. 2018 for details). As a result, this normal part was not included in their final stratigraphic interpretation. In addition, the ostracod fauna from the clay pit Mitterdorf has been investigated by Brinkmann et al. (2019). These authors found that, compared to the foraminifers, the ostracods appeared to point to a slightly younger age for Mitterdorf, namely the transition from lower to middle Ottnangian.

In July 2019, the outcrop had been significantly extended and levels not accessible in 2014 and 2015 could be investigated. For the sake of completeness, we sampled the entire succession for paleomagnetic analysis, resulting in 36 samples covering a stratigraphic thickness of ~ 18 m.

**Outcrop Türkenbach** This outcrop is located along the Türkenbach, a stream near the town of Stammham am Inn

(48°14′48.5″ N; 12°54′10.1″ E). It is close to the classical Türkenbach site of the Onc Fm (Reichenbacher 1993), which has since become completely overgrown. In 2016, a catastrophic flood created the new outcrop, approximately 200 m upriver from the classical site. It exposes an 8 m thick section of the Onc Fm, which we sampled for magnetostratigraphic analyses at 16 levels.

**Borehole Füssing-TH1** A drilling near the town of Füssing (48°21′18.6″ N; 13°18′47.6″ E) was carried out in the course of a geothermal project by Piewak and Partner (Bayreuth). A total of 59 samples (1 kg each) from the upper 95 m of the borehole were included in our study.

**Borehole Simbach** The drilling was located near the town of Simbach am Inn (48°16′20.1″ N; 13°2′55.6″ E). In the context of an engineering geology, the company Müller and Hereth (Karlsruhe) extracted 40-m long drilling cores. We obtained three samples (2 kg each) from depths of 11.4 m, 21.4 m, and 38.8 m of the core designated BK-07-TU-2018-GWM.

### Published data

**Borehole data** Lithostratigraphic data from a total of 148 drillings were compiled from the following sources:

- Data from 107 boreholes were accessed from the website of the Bavarian Environmental Agency (Bayerisches Landesamt für Umwelt, LfU) http://www.umweltatlas.bayern.de/mapapps/resources/apps/lfu_geologie_ftz/index.html?lang=de.
- Data from eight boreholes were available from publications, i.e., Taufkirchen 1 (Knipscheer 1952); VB1 Aigner Forst, VB2 Osterholzen (Wenger 1993); Simbach-Braunau Thermal 1/S-B Th1 (Goldbrunner et al. 2001); Ortenburg CF 1001, CF 1002, CF 1003 (Hagn 1953); and Straß (Pippèrr and Reichenbacher 2009).
- Stratigraphic data from 33 boreholes conducted by oil companies were assembled from the archive maintained by the LfU.

**Outcrop data** Lithostratigraphic data from the historical outcrop Maierhof, stratotype for the 'Ortenburg Meeressand', were recorded from Hagn et al. (1981). Litho- and biostratigraphic information and polarity data for magnetostratigraphy of four still accessible outcrops (Untersimbach, Neuhofen, Beham and Prienbach) were taken from Pippèrr et al. (2018).

**Outcrop data for the 'Shell bed horizon'** One important marker bed in the lower Onc Fm is a shell bed horizon ('Schillhorizont' in the German literature), which is almost exclusively composed of the shells of the brackish bivalve *Rzehakia guembeli* (Schlickum and Strauch 1968; Schneider et al. 2011). We assembled altitude data (m.a.s.l.) for the basis of this horizon from a total of 30 outcrops described by Mayr (1957), Grimm (1963), Schlickum and Strauch (1968) and Schneider et al. (2011).

## Methods

### Lithostratigraphy and micropalaeontology

Profile logging and, where possible, macrofossil collection were conducted to determine the lithofacies and lithostratigraphy. Taxonomic identification of macrofossils was done using comparative material from collections kept in the Bavarian State Collection of Palaeontology and Geology and previous descriptions (Schlickum 1964; Binder 2004; Kowalke and Reichenbacher 2005).

Recognition of lithostratigraphic units in boreholes through the OMM benefits greatly from micropalaeontological analysis. Bulk samples from the boreholes Füssing TH 1 and Simbach were processed using standard techniques for micropalaeontological analyses (Pippèrr 2011); sieve mesh sizes were 63 µm, 200 µm, 400 µm and 630 µm. Microfossils were picked under a reflected-light microscope (Leica MZ6) and systematically sorted. For the taxonomic identification of foraminifers, we consulted Wenger (1987), Cicha et al. (1998), Rupp and Haunold-Jenke (2003), Roetzel et al. (2006), Pippèrr and Reichenbacher (2009, 2010), Pippèrr (2011) and ter Borgh et al. (2014). For planktonic foraminifers, Rögl (1994) was particularly useful, while Hofmann (1967) facilitated species identification of *Bolivina*. Literature sources used for ostracod identification included Oertli (1956), Witt (2000, 2009), and Brinkmann et al. (2019).

### Magnetostratigraphy

Standard paleomagnetic cores were drilled from 36 levels of the Mitterdorf clay pit (Fig. 5a) and 16 levels of the Türkenbach section (Fig. 6a). The paleomagnetic analyses were carried out at the Paleomagnetic laboratory at Tübingen University (Mitterdorf) and the Paleomagnetic Laboratory 'Fort Hoofddijk' at Utrecht University in the Netherlands (Türkenbach). For Mitterdorf, 19 samples were treated with alternating field (AF) and 18 samples with thermal demagnetization procedures using the 2-G automatic long-core sample handler and the ASC thermal demagnetizer (http://ascscientific.com). For Türkenbach, a total of 15 samples were treated with AF demagnetization (15 steps from 0 to 80 mT) by means of a custom-built automated system (Mullender et al. 2016). The magnetization in both laboratories was measured in three components at each demagnetization

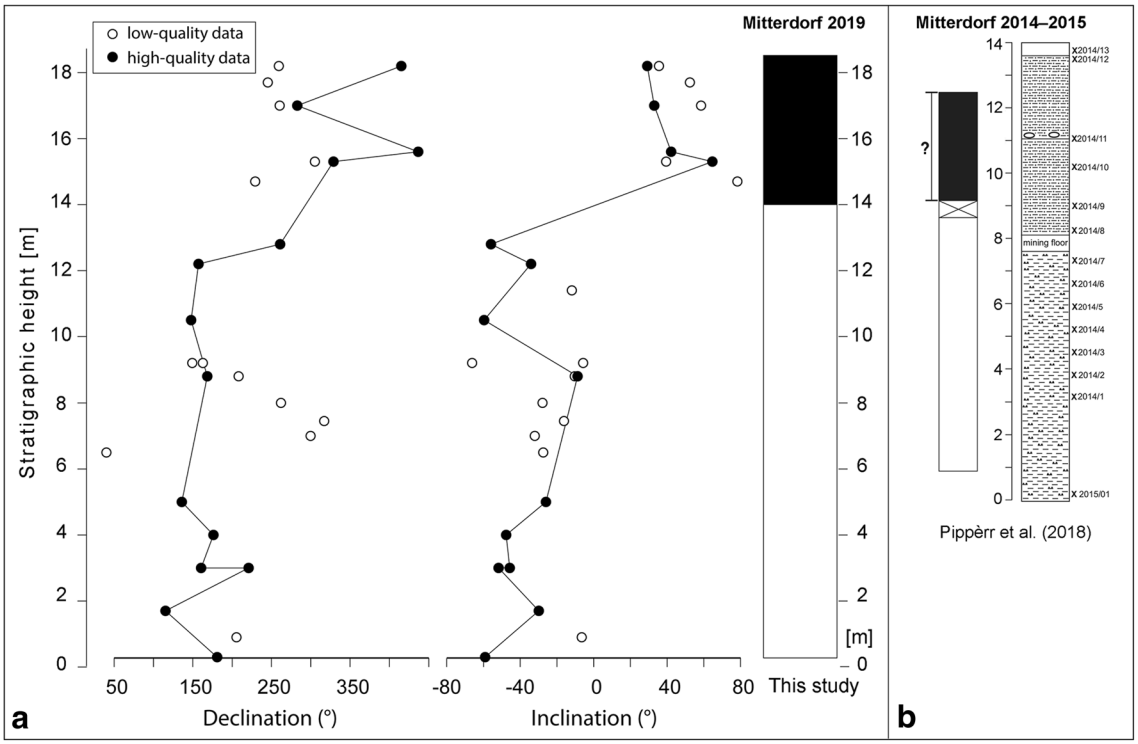


**Fig. 5** **a** Paleomagnetic results for the Neuhofen Fm at the Mitterdorf outcrop showing declination and inclination of the least-squares method versus the stratigraphic height of the section and corresponding polarity data (white = reverse; black = normal). Filled and open dots represent high and low quality results, respectively. **b** Log of the section and polarity data derived from the Neuhofen Fm at Mitterdorf in 2014 and 2015 (modified from Pippèrr et al. 2018)

step with a 2G Enterprises DC SQUID magnetometer (noise level: $3 \times 10^{-12}$ A m$^2$). Interpretation of the demagnetization directions was done in Paleomagnetism.org (Koymans et al. 2016). Here, the linear segments of the orthogonal projections of the data (Zijderveld 1967) were quantified with a least-squares method (Kirschvink 1980; McFadden and McElhinny 1988).

### Three-dimensional (3D) geological modeling

Basic data comprised information from the 150 drilling sites reported above and included for each borehole (1) name or ID number, (2) coordinates, (3) altitudes for top (ground surface) and bottom of the borehole, (4) vertical drilling depth, and (5) top and base of each of the lithostratigraphic units included in the model (see Supplementary Material). All data were compiled in Microsoft Excel (Version 7.4.1), transformed into a ".csv" format, and then imported into QGIS (2.14 Essen), an open source geoinformation system. QGIS operates mainly with plug-in tools. The plug-in "Midvatten" transforms the dataset into a database, connecting different properties such as altitudes of strata boundaries, coordinates and generating a color ramp. A digital elevation model (DEM) of the present-day topography (m.a.s.l.) served as a base map; its resolution is 50 m (one pixel). DEMs were produced for the bases of nine lithostratigraphic units (OMM, 'Ortenburg Meeressand', US Fm, NH Fm, Li HH, GS-BM, Onc Fm, 'Ortenburg Schotter', OSM) by interpolating all data points containing the altitude (m a.s.l.) of the respective base using the Interpolation tool. Due to the linear interpolation, the DEMs provide a somewhat simplified view of the geological situation. Cross sections were prepared on the basis of the DEMs using the Terrain Profile plug-in; borehole profiles and outcrops that intersect with the respective cross section were then added. Tectonic structures (faults) were taken from geological maps and the literature (Unger and Schwarzmeier 1982), and their intersections with the modeled strata were marked in 3D. The cross sections depict dipping directions and vertical throws of faults based on the geological interpretation of the raw data. DEMs of six lithostratigraphic units (OMM, US Fm, NH Fm, GS-BM, Onc Fm, OSM) were additionally used to extract isolines (depth maps) for the strata bases using the Contour tool.

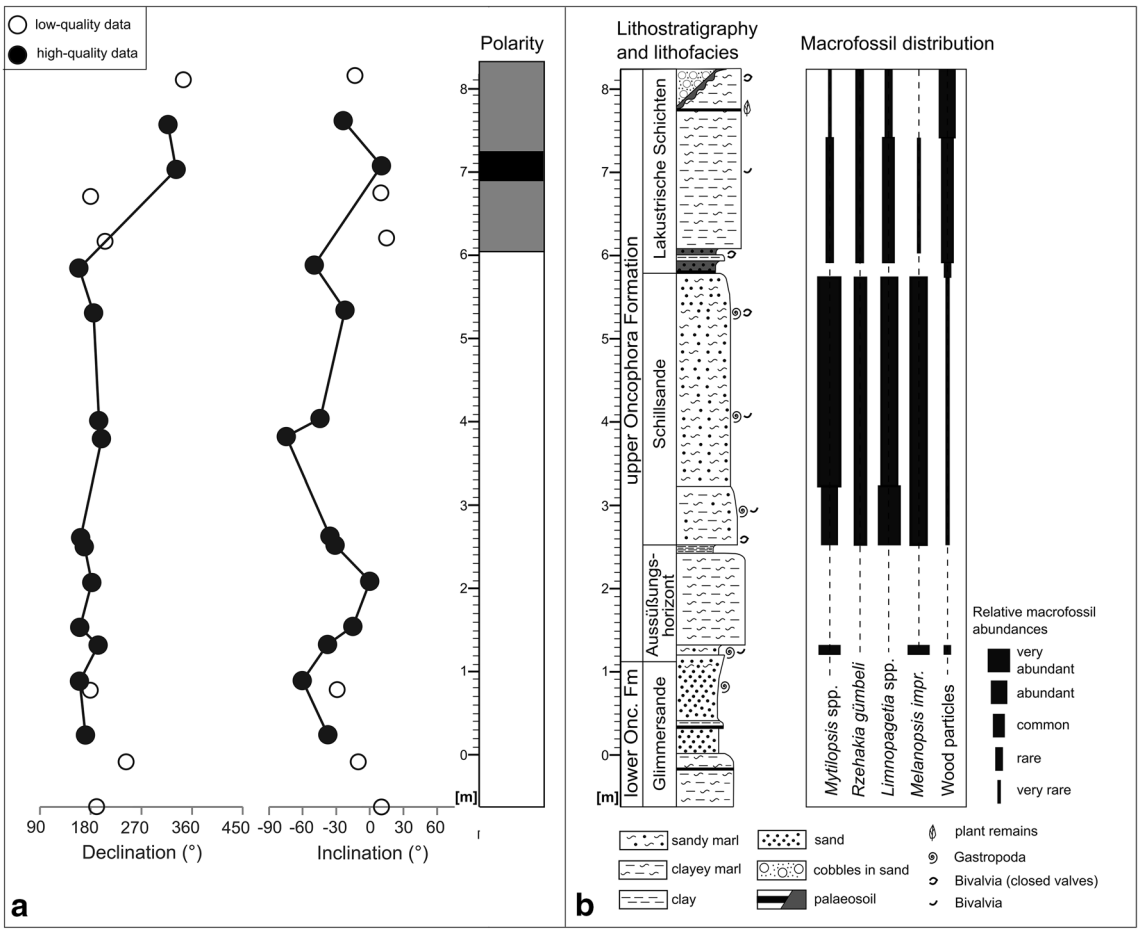


**Fig. 6** **a** Paleomagnetic results for the Oncophora Fm of the Türkenbach outcrop showing declination and inclination of the least squares method versus the stratigraphic height of the section and corresponding polarity data (white = reverse; black = normal). **b** Lithostratigraphy, lithofacies and macrofossil content of the same profile of the Oncophora Fm at the outcrop Türkenbach

## Results

### Stratigraphy

#### Outcrop Mitterdorf

The 18-m section is made up of marls and marly clays with variable abundances of silt and sand layers; few macrofossils (bivalves, gastropods) were found. With the exception of the lowermost portion (4 m), which was newly uncovered by the ongoing mining, the section corresponds to the NH Fm exposed in 2014 and 2015 (see Pippèrr et al. 2018 and Fig. 5a, b). Microfossil data confirmed that the characteristic foraminiferal assemblage of the NH Fm is also present in the newly accessible lowermost part of the section.

The magnetostratigraphic measurements revealed weak but stable demagnetization behavior, similar to the results presented by Pippèrr et al. (2018) from the same outcrop. Generally thermal treatment yielded high-quality results with a clear trend toward the origin of the projection plane, whereas AF demagnetization was more difficult to interpret. An overall trend, with the top part being of normal polarity (18–14 m) and the lower part being of reversed polarity (14–0 m), is nevertheless evident (Fig. 5a). This result is in principle similar to that reported in Pippèrr et al. (2018) (Fig. 5b), but extends the thickness of the reverse portion and confirms the normal polarity of the upper part.

#### Outcrop Türkenbach

The 8-m section revealed by this outcrop is made up of sandy, silty, marly and clayey sediments with variable abundances of macrofossils (Fig. 6b). Bivalves are often preserved with both valves, thus indicating an autochthonous fossil assemblage. Based on the lithofacies and abundances of the bivalves *Rzehakia gümbeli*, *Mytilopsis* and *Limnopagetia* and the gastropod *Melanopsis*, four of the seven horizons of the Onc Fm can be recognized (from bottom to top): 1.10 m 'Glimmersande' [Sand with mica], 1.40 m 'Aussüßungshorizont' [Freshwater horizon], 3.25 m

'Schillsande' [Shell bed sand], and 2.45 m 'Lakustrische Schichten' [Lacustrine beds]. Accordingly, the Türkenbach section exposes the top of the lower Onc Fm ('Glimmersande') and almost the whole of the upper Onc Fm (Fig. 6b).

The magnetostratigraphic measurements revealed that the majority of the samples show a stable behavior, with a decay toward the origin in the Zijderveld diagrams (Zijderveld 1967). Lower field components (of normal polarity) were present in the interval 0–15 mT for some samples, while the higher field component was usually visible between 25 and 50 mT. Thirteen specimens were of high quality (closed circles in Fig. 6a), six specimens were of lower quality (i.e., noisier; open circles in Fig. 6a), and most of the samples could be used for interpretation of the magnetic polarity. In summary, the Türkenbach section displays reversed polarity up to 6 m (Fig. 6b). The uppermost meter (7–8 m) yielded a sample of mixed polarities (i.e., normal declination, reversed inclination) and one of normal polarity. The latter did not have a lower field component, so it is likely that the top of the section represents a normal overprint.

#### Borehole Füssing-TH1

The sediments are marly to silty. Microfossils are abundant and usually very well preserved, as fragile structures such as ostracod spines are present and the shells show no signs of corrosion. Benthic foraminifers make up the most abundant group, comprising 41 species and about 5230 specimens (a species list is provided in Table 1). Species diversity ranges from 8 to 22 taxa per sample (Table 1). Planktonic foraminifers mainly consist of three species (or species groups), i.e., *Tenuitella angustiumbilicata*, *Ciperoella ciperoensis/C. anguliofficinalis,* and *Globigerinella obesa*, with *T. angustiumbilicata* being the most abundant overall (114 individuals). Note that *C. ciperoensis* and *C. anguliofficinalis* are the new taxonomic interpretations of what was previously described as *Globigerina ciperoensis* and *G. ottnangiensis* (Olsson et al. 2018). *Globigerinella obesa* is the revised name of *Globorotalia obesa* (Spezzaferri et al. 2018), and *Tenuitella* is considered to include the form-genus *Tenuitellinata*, to which the species *angustiumbilicata* had been referred in previous work (Pearson et al. 2018).

Relative abundances of benthic and planktonic foraminifers differ in the samples, as seen in the variable plankton/benthos (P/B) ratios (Fig. 7). Spines of echinoids, ostracods and fish otoliths are also moderately common to abundant. Rare microfossil remains include sponge spicules, gastropods, bryozoans, and teeth of sharks and rays.

The characteristic microfossil assemblages allowed us to assign the interval from 95 to 57 m to the US Fm and the interval above it to the NH Fm. In the US Fm, the dominant element of the benthic foraminiferal assemblage is *Lenticulina* spp., which account for up to 90% of the foraminifer specimens (Fig. 7). Other notably common benthic foraminifers are *Cibicidoides* spp. and in the lowermost samples also *Nonion commune*; all other species are scarce (Table 1). This assemblage fully conforms to the composition that is characteristic for the US Fm (Wenger 1987; Pippèrr 2011; Pippèrr et al. 2018). At the boundary with the NH Fm, the composition of the benthic foraminiferal assemblage undergoes a clear change (Fig. 7). *Lenticulina* spp., though still abundant, is now less dominant. The fraction of *Astrononion perfossum* specimens increases markedly from $< 10$ to $> 40\%$. From 57–20 m, the NH Fm is further characterized by abundant occurrences of *Sigmoilopsis ottnangensis, Spiroplectammina pectinata,* and *Caucasina cylindrica/C. schischkinskayae,* and also of the ostracods *Carinovalva neuhofensis* and *Loxoconcha linearis.* The co-occurrence of these species is typical for the NH Fm (Wenger 1987; Witt 2009). The samples from 20 to 8 m show a distinct reduction in the abundance of the benthic foraminifers, with specimen numbers dropping by 50% (or more) relative to the underlying samples (Table 1; Fig. 7). Notably, the numbers of species present remain more or less unchanged, except for the lack of *Spiroplectammina pectinata*. P/B ratios are considerably higher than before and reach their maximum (45.5%) near the top of the borehole (Fig. 7). We interpret the interval from 20 to 8 m as part of the NH Fm because it contains with *Sigmoilopsis ottnangensis* a typical element of the NH Fm, and lacks *Ammonia beccarii*, which is usually present in the GS-BM (see Wenger 1987; Pippèrr 2011).

#### Borehole Simbach

The sediments consist of light gray, silty marls alternating with silts and fine- to medium-grained glauconitic sands. The samples contained large amounts of siliceous microfossils (sponge spicules) and echinoid spines, but relatively few foraminifers, ostracods and otoliths (Table 2). Their preservation is moderate, and shells and tests are mostly corroded. Benthic foraminifers comprise 13 taxa, and *Nonion commune* and *Ammonia beccarii* are comparatively abundant. Ostracods are represented by three taxa and the otoliths signal the presence of juvenile gobiids only. Both the lithofacies and the microfossil assemblage clearly indicate that the sampled intervals are part of the GS-BM (Wenger 1987; Pippèrr 2011).

### Results derived from the 3D geological model

#### Depth maps

The depth maps for the bases of the OMM, US Fm, NH Fm and GS-BM reveal that the elevation (in m.a.s.l.) of each base generally increases from south–southwest to northeast—the OMM base from $-625$ to $+350$ m (Fig. 8a),

**Table 1** Species list for the borehole Bad Füssing

| Depths interval (m) | 6–11 | 12–17 | 18–25 | 26–34 | 35–40 | 41–49 | 51–55 | 57–61 | 63–73 | 75–85 | 87–95 | *n* |
|---|---|---|---|---|---|---|---|---|---|---|---|---|
| Benthic foraminifera | | | | | | | | | | | | |
| *Semivulvulina pectinata* (Reuss, 1850) | | | 18 | 122 | 90 | 73 | 20 | 5 | 4 | 8 | 14 | 334 |
| *Quinqueloculina buchiana* d'Orbigny, 1846 | | | 1 | 21 | 27 | 9 | | 1 | | | | 59 |
| *Sigmoilinita tenuis* (Čžjžek, 1848) | 2 | 1 | 1 | 1 | 1 | | | | | | 1 | 7 |
| *Sigmoilopsis ottnangensis* Cicha, Čtyroká & Zapletalova, 1973 | 3 | 26 | 42 | 86 | 95 | 114 | 41 | 11 | 3 | 4 | 12 | 437 |
| *Lenticulina inornata* (d'Orbigny, 1846)/*L. melvilli* (Cushman & Renz, 1941) | 39 | 133 | 117 | 300 | 347 | 244 | 236 | 435 | 327 | 246 | 522 | 2946 |
| *Lenticulina cultrata* (Montfort, 1808) | | 1 | 1 | 10 | 11 | 2 | | | | | | 25 |
| *Saracenaria* cf. *arcuata* (d'Orbigny, 1846) | 1 | 1 | 2 | 2 | 1 | 5 | 2 | 1 | | | 3 | 18 |
| *Astacolus crepidulus* (Fichtel & Moll, 1798) | | | | | 1 | | | | | 1 | | 2 |
| *Laevidentalina communis* (d'Orbigny, 1826) | 1 | 12 | 8 | 17 | 11 | 8 | 2 | | | | 3 | 60 |
| *Amphimorphina haueriana* Neugeboren, 1850 | | | | | 3 | 9 | 2 | | | | | 14 |
| *Amphicoryna ottnangensis* (Toula, 1914) | 2 | 10 | 11 | 10 | 24 | 54 | 11 | 11 | 1 | 1 | 1 | 136 |
| *Lagena striata* (d'Orbigny, 1839) | | | | 3 | | 3 | 2 | 1 | | | | 9 |
| *Lagena laevis* (Montagu, 1803) | | | | | 1 | 4 | 2 | 2 | | | | 9 |
| *Globulina gibba* (d'Orbigny in Deshayes, 1832) | | 1 | | 1 | | | | | | | | 2 |
| *Bulimina striata* d'Orbigny in Guérin-Méneville, 1832 | | | | | | | | | | | 1 | 1 |
| *Virgulopsis tuberculata* (Egger, 1857) | | | | 1 | | | | | | | | 1 |
| *Caucasina cylindrica* Zapletalova, 1973/*C. schischkinskayae* (Samoilova, 1947) | 1 | 7 | 19 | 79 | 16 | 19 | 10 | 1 | | | 6 | 148 |
| *Fursenkoina acuta* (d'Orbigny, 1852) | | | 2 | 4 | | 8 | 16 | 19 | | | 2 | 51 |
| *Bolivina dilatata* Reuss, 1850 | 1 | 9 | 6 | 2 | 4 | | | | | | | 22 |
| *Bolivina scitula* Hofmann, 1967 | 1 | 6 | 1 | 3 | | | | | | | 1 | 12 |
| *Bolivina concinna* (Knipscheer & Martin, 1955) | | | 1 | | | | | | | | | 1 |
| *Bolivina crenulata trunensis* Hofmann, 1967 | | | | | | | | | 1 | | | 1 |
| *Fissurina orbignyana* Seguenza, 1862 | | | | | 1 | | | | | | | 1 |
| *Elphidium ortenburgense* (Egger, 1857) | | | | | 1 | | | | | | | 1 |
| *Elphidium flexuosum flexuosum* (d'Orbigny, 1846) | | | | | | | | 1 | 1 | | | 2 |
| *Elphidium flexuosum subtypicum* Papp, 1963 | | | | | | | | | 1 | | | 1 |
| *Elphidiella minuta* (Reuss, 1865) | | 1 | | | | | | | | | | 1 |
| *Elphidiella cryptostoma* (Egger, 1857) | | | | | 1 | | | | | | | 1 |
| *Protelphidium roemeri* (Cushman, 1936) | | 13 | 8 | 1 | | | | 1 | | 1 | | 24 |
| *Nonion commune* (d'Orbigny, 1846) | 1 | | 3 | 1 | | 2 | | 2 | 3 | 4 | 12 | 28 |
| *Astrononion perfossum* (Clodius, 1922) | 1 | 5 | 22 | 38 | 32 | 151 | 238 | 36 | 1 | 1 | 21 | 546 |
| *Melonis pompilioides* (Fichtel & Moll, 1798) | | | | | 3 | 27 | 4 | 1 | 2 | | 1 | 38 |
| *Ammonia beccarii* (Linnaeus, 1758) | | | | 2 | | | | | 1 | | | 3 |
| *Discorbis biaperturata* Pokorný, 1956 | | 1 | 1 | | | | | | | | | 2 |
| *Gyroidina parva* Cushman & Renz, 1941 | | | | | | | | | | | 5 | 5 |

**Table 1** (continued)

| Depths interval (m) | 6–11 | 12–17 | 18–25 | 26–34 | 35–40 | 41–49 | 51–55 | 57–61 | 63–73 | 75–85 | 87–95 | *n* |
|---|---|---|---|---|---|---|---|---|---|---|---|---|
| *Charltonina tangentialis* (Clodius, 1922) | | 6 | 5 | 4 | 7 | 10 | 16 | 3 | | | 3 | 38 |
| *Oridorsalis umbonatus* (Reuss, 1851) | | 3 | 18 | 6 | 7 | 8 | 2 | | | | 1 | 43 |
| *Cibicides lobatulus* (Walker & Jacob, 1798) | | 2 | 5 | 6 | 6 | 2 | | 1 | | 1 | 1 | 24 |
| *Cibicidoides lopjanicus* (Myatlyuk, 1950)/*C. tenellus* (Reuss, 1865) | | 11 | 12 | 18 | 9 | 27 | 2 | 6 | 6 | 11 | 23 | 125 |
| *Heterolepa dutemplei* (d'Orbigny, 1846) | 1 | | 2 | 2 | | 1 | | | | 1 | 1 | 8 |
| *Hanzawaia boueana* (d'Orbigny, 1846) | | 5 | | 3 | | | | | 2 | | 3 | 13 |
| Planktonic Foraminifera | | | | | | | | | | | | |
| *Ciperoella ciperoensis* (Bolli, 1954)/*C. anguliofficinalis* (Blow, 1969) | 4 | 6 | 21 | 9 | 10 | 8 | | | 2 | 3 | 12 | 75 |
| *Tenuitella angustiumbilicata* (Bolli, 1957) | 20 | 20 | 14 | 10 | 9 | 5 | 2 | | 6 | 7 | 21 | 114 |
| *Globigerinella* cf. *obesa* (Bolli, 1957) | 2 | 1 | 3 | | | | 1 | | 5 | 1 | 12 | 25 |
| *Praeorbulina* spp. | | 6 | 2 | | 2 | 2 | | | | 1 | | 13 |
| Planktonic Foraminifera indet. | 19 | 58 | 34 | 20 | 24 | 15 | 1 | | 14 | 3 | 36 | 224 |
| Total number foraminifer specimens | 99 | 345 | 380 | 782 | 744 | 810 | 610 | 538 | 380 | 294 | 718 | 5700 |
| Total number foraminifer species | 16 | 25 | 28 | 29 | 27 | 25 | 19 | 18 | 17 | 16 | 25 | 47 |
| Planktonic/Benthic ratio (%P) | 45.5 | 26.4 | 19.5 | 5 | 6.1 | 3.7 | 0.7 | 0 | 7.1 | 5.1 | 11.3 | 7.9 |
| Ostracoda | | | | | | | | | | | | |
| *Cytherella* sp. | | 2 | | 3 | 8 | 4 | 3 | 1 | | | | 21 |
| *Cytherella* aff. *méhesi* Brestenská, 1975 | | | | | 2 | 1 | 1 | 1 | | | | 5 |
| *Costa* sp. | | | | 1 | 2 | 5 | 5 | 2 | | | | 15 |
| *Carinovalva neuhofenensis* (Witt, 1967) | | | 5 | 24 | 14 | 4 | 5 | | | | | 52 |
| *Pterygocythereis ceratoptera* (Bosquet, 1852) | | 1 | | 4 | 7 | | | | | | | 12 |
| *Loxoconcha eggeriana* Lienenklaus, 1897 | | | | | 1 | | | | | | | 1 |
| *Loxoconcha* cf. *linearis* Carbonnel, 1969 | 5 | 23 | 14 | 31 | 46 | 3 | 3 | | 1 | 1 | | 127 |
| *Cytheropteron* sp. | | | | 1 | | | | | | | | 1 |
| Ostracoda indet. | | | | 2 | | 1 | | | | | | 3 |
| Fish bones and teeth indet | 2 | 5 | 1 | 8 | 10 | 2 | 2 | 1 | | | | 31 |
| Fish otoliths | | | | | | | | | | | | |
| *Diaphus* sp. | 1 | | | | 4 | 1 | | | | | | 6 |
| *Diaphus austriacus* (Koken, 1891) | | | | 1 | 2 | 2 | | | | | | 5 |
| *Notoscopelus* sp. | | | | | 1 | | | | | | | 1 |
| *Bathygadus* sp. | 1 | | 1 | | | | | | | | | 2 |
| *Phycis* sp. | | | | 1 | | | | | | | | 1 |
| *Pomadasys* sp. | | | 1 | | | | | | | | | 1 |
| Selachii | | | | | | | | | | | | |
| Teeth indet | | 2 | 1 | 1 | 1 | 1 | | | | | | 6 |
| Denticles indet | | | 1 | 1 | | | | | | | | 2 |

**Table 1** (continued)

| Depths interval (m) | 6–11 | 12–17 | 18–25 | 26–34 | 35–40 | 41–49 | 51–55 | 57–61 | 63–73 | 75–85 | 87–95 | *n* |
|---|---|---|---|---|---|---|---|---|---|---|---|---|
| *Squalus* sp. | | | | 1 | | | | | | | | 1 |
| Batoidea teeth/denticles | | | | 2 | | | | | | | | 2 |
| Gastropoda | | | | | | | | | | | | |
| cf. *Bithynia* sp | 1 | | | | | | | | | | | 1 |
| *Acteon* sp. | | | | 3 | 1 | 2 | | | | | | 6 |
| Gastropoda indet. | 2 | 3 | 5 | 3 | 11 | 3 | | 1 | 1 | | | 29 |
| Echinoidea (spines) | 4 | 53 | 66 | 72 | 87 | 83 | 8 | 8 | 7 | 1 | 4 | 393 |
| Porifera (Demospongiae and Hexactinellida) | 1 | 1 | 2 | | 2 | 1 | | 1 | | | 2 | 10 |
| Bryozoa | | | | 2 | | | | | | | | 2 |

P/B ratio of foraminifera, total number of specimens and taxa at a certain depth, as well as the total number of each identified species are also shown. Note that sampled depths are fused, as each data point represents a combination of data from six samples

the US Fm base from − 125 to + 250 m (Fig. 8b), the NH Fm base from − 275 to + 325 m (Fig. 8c), and the GS-BM base from − 25 to + 375 m (Fig. 8d). The inclination usually ranges from 3° to 4° (bases OMM, US Fm, NH Fm) to 2° (base GS-BM); it is smallest in the northeast. The base of the OMM is deepest in the southern area of the Landshut–Neuötting High; the dip is steepest here and oriented to the south (Fig. 8a). The base of the US Fm is deepest in the southern Braunau Trough, but its extension further to the Landshut–Neuötting High is unknown (Fig. 8b). The bases of NH Fm and GS-BM show a similar pattern like the base of the OMM, but steep dipping is additionally recognizable in the southern Braunau Trough (Fig. 8c, d). The base of the Onc Fm rises from west-southwest to east–northeast, from + 200 to + 400 m (Fig. 8e). Again, the steepest inclination is seen in the southern area of the Landshut–Neuötting High; outside this region, the dip is very shallow (about 1°) and becomes almost horizontal in the middle of the Braunau Trough (Fig. 8e). The altitude of the base OSM increases from southwest to southeast/east from + 200 to + 475 m; the bedding is almost horizontal in the Braunau Trough and slightly steeper to the southwest in the area of the Landshut–Neuötting High (Fig. 8f).

In summary, the depth maps indicate that both the Landshut–Neuötting High and Braunau Trough were prominent sectors of subsidence, but that the subsidence of the Braunau Trough ceased in the course of the GS-BM deposition. In the distal sector of the study area in the northeast, near Passau and the Bohemian Massif, the rates of subsidence were low throughout the interval of interest as indicated by the shallow-to-absent dip of all modeled bases.

### Cross sections

The cross sections shown in Figs. 9 and 10a illustrate that the strata studied here were deposited largely isochronously. A palaeorelief is recognisable at the base of the US Fm, as the US Fm fills a depression within the older Eggenburgian sediments in the northern Braunau Trough (Profile B) and in the easternmost part of the Aidenbach–Griesbach High (Profile A). Both the US Fm and NH Fm have a relatively constant thickness in west–east direction; the thickness of the GS-BM slightly increases to the west, and the thickness of the Onc Fm rises slightly to the east (Profile A, Fig. 9). That the OSM increases in thickness toward the west is a consequence of the erosion (see below). In north–south direction, the thicknesses of the NH Fm, GS-BM and Onc Fm increase slightly, while the thickness of the US Fm varies and is highest in the central-to-southern Braunau Trough and in the southern area of the Aidenbach–Griesbach High (Profiles B–D, Figs. 9, 10a). The variable thickness of the US Fm could indicate that a phase of erosion happened after its deposition. However, in many previous works, the US

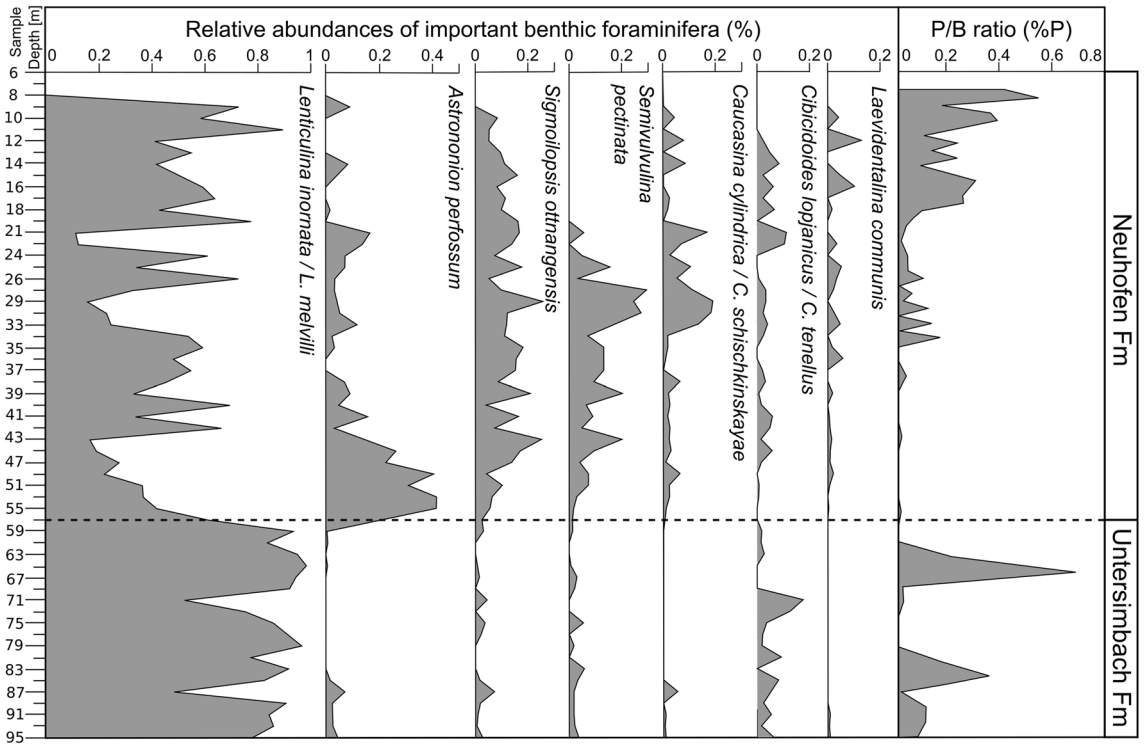


**Fig. 7** Distribution of the most abundant benthic foraminifers and pattern of the planktonic to benthic (P/B) ratio in the Untersimbach Fm and Neuhofen Fm based on the drill core Füssing TH-1. Note that drilling depths are shown not to scale due to the selection of sampling intervals

Fm was considered to be part of the NH Fm and was not recognized as a distinctive unit (Wenger 1987; Pippèrr et al. 2018). Although we checked all borehole data carefully in this respect, we cannot exclude that the varying thicknesses of the US Fm are a result of the problem to designate this unit accurately solely based on lithological data.

Furthermore, the 3D model reveals a distinctive facies in the north, on the Aidenbach–Griesbach High (Profile B). There, the US Fm is absent, the NH Fm and lower part of the GS-BM are replaced by the 'Littoral facies of Holzbach and Höch', while the uppermost GS-BM and lowermost Onc Fm are replaced by the fluvial 'Ortenburg Schotter'. Notably, the 'Littoral facies of Holzbach and Höch' replaces the lowermost GS-BM also in the small graben structure that occurs in the eastern Braunau Trough (see Profile A and B).

Faults caused vertical throws of the bases of all lithostratigraphic units of the OMM. Most faults terminate within the GS-BM; only the faults bounding the Braunau Trough also displaced the base of the Onc Fm (Profiles A and C). The OSM lies uniformly above the Onc Fm.

### Intersection of outcrops with the 3D model

The cross sections of Profile C and D visualize the intersection of outcrops with the 3D model (Fig. 10a). The outcrops involved are Mitterdorf and Türkenbach (this study, Figs. 5, 6) and Untersimbach, Neuhofen, Beham and Prienbach from Pippèrr et al. (2018). Profile C reveals that the Türkenbach outcrop belongs to the upper Onc Fm, as we had assumed on the basis of its lithofacies and fossils. Profiles C and D demonstrate that the outcrops Untersimbach, Mitterdorf, Beham and Prienbach each occur in a lithostratigraphic position that corresponds with the interpretation of Pippèrr et al. (2018). The main difference concerns the outcrop Neuhofen (see Profile D), which was considered by them to represent the lower NH Fm, not distant from the top of the US Fm. The 3D model shows, however, that Neuhofen is located in the *upper* NH Fm, and is underlain by a further 80 m of NH Fm; only then does the US Fm appear (Fig. 10c). The revised position of the Neuhofen outcrop forces a re-interpretation of its magnetostratigraphic data (see below).

## Discussion

### Note on the siliceous microfossils from the Simbach core

The samples from the Simbach borehole contained large amounts of siliceous sponge spicules. Siliceous microfossils are usually rare or absent in OMM sediments; however, informative records (diatoms) are known from

**Table 2** List of microfossils for the borehole Simbach and total number of taxa at a certain depth

| Depth (m) | 11.4 | 21.4 | 38.8 |
|---|---|---|---|
| Foraminifera | | | |
| Number of taxa | 5 | 4 | 10 |
| *Textularia gramen* d'Orbigny, 1846 | | | 2 |
| *Quinqueloculina* sp. | 1 | | |
| *Stilostomella perscripta* (Egger, 1857) | | | 1 |
| *Globulina gibba* (d'Orbigny in Deshayes, 1832) | | | 2 |
| *Bolivina dilatata* Reuss, 1850 | | | 1 |
| *Elphidium glabratum* Cushman, 1939 | | | 1 |
| Cf. *Elphidiella minuta* (Reuss, 1865) | | | 1 |
| *Protelphidium roemeri* (Cushman, 1936) | 1 | | |
| *Nonion commune* (d'Orbigny, 1846) | 1 | 2 | 1 |
| *Ammonia beccarii* (LINNÉ) | 5 | 4 | 3 |
| *Cibicidoides tenellus* (Reuss, 1865) | | 1 | 1 |
| *Hanzawaia boueana* (d'Orbigny, 1846) | | 1 | |
| Planktonic (*Ciperoella* spp.) | 1 | 2 | 5 |
| Foraminifera indet. | 1 | | |
| Ostracoda | | | |
| *Cytheridea acuminata* Bosquet, 1852 | 4 | | 5 |
| *Loxoconcha eggeriana* Lienenklaus, 1896 | 4 | | |
| *Costa* sp. | 7 | 1 | |
| Ostracoda indet. | 3 | 1 | 2 |
| Fish remains | | | |
| Gobiidae juv. sp. (otolith) | | | 1 |
| Fish bones indet. | 3 | | 1 |
| Gastropoda | | | |
| Gastropoda indet. | 3 | 7 | 1 |
| Echinoidea (spines) | x | x | x |
| Porifera (Demospongiae and Hexactinellida) | xx | x | xx |

southern Germany, Upper and Lower Austria. In southern Germany and Upper Austria, diatoms are very abundant in the lower Achen Fm (Pippèrr et al. 2007) and Ried Fm (Rupp et al. 2008), respectively. Each of these formations is interpreted as a stratigraphic equivalent of the GS-BM (Pippèrr and Reichenbacher 2017; Pippèrr et al. 2018). In Lower Austria, mass occurrences of diatoms appear in the Zellerndorf Fm (Roetzel et al. 2006; Grunert et al. 2010). An ash layer with a $^{40}Ar/^{39}Ar$ age of $17.23 \pm 0.18$ Ma overlies the Zellerndorf Fm, which is thus of Ottnangian or early Karpatian age (Roetzel et al. 2014). This abundance of siliceous microfossils has been attributed to upwelling conditions due to deepening of the NAFB (Roetzel et al. 2006; Pippèrr et al. 2007; Grunert et al. 2010). Together with the volcanism (Roetzel et al. 2014), they may record one or two isochronous deepening events across the NAFB, but further studies are needed to confirm this suggestion.

## Evaluation of the 3D geological model

Several lines of evidence indicate that the computer-generated geological model presented here is of high quality: (1) the modeled bases of the OMM and NH Fm are in complete agreement with the depth maps assembled by the GEOMOL project, which partially overlap with our study area (Gusterhuber et al. 2012; Pfleiderer et al. 2016; http://maps.geomol.eu); (2) the modeled strata intersect fully with the mapped surface geology (GK 25, Unger 1984; GK 500, Geological Map of Bavaria), as well as with previously described outcrops (Unger 1984; Pippèrr et al. 2018); and (3) the small-scale distribution of the 'Ortenburg Schotter' is consistent with published data (Unger 1982; Diepolder et al. 2011). The large number of data points used to build the model (see Fig. 4) further strengthens its quality.

Overall, the results of the 3D model are largely consistent with the results of previous work in the study area, but the differences nevertheless provide new insights. The most significant differences concern the maximal thicknesses of certain formations. The modeled thickness of the NH Fm reaches 280 m in the south of the study area (Profile C) vs. 220 m described by Unger (1984), while that of the GS-BM reaches 200 m in the southern Braunau Trough (Profiles B and C) vs. 80 m recorded by Unger (1984). The model also suggests a greater thickness for the Onc Fm (50–100 m) than that previously reported (15–45 m, Schlickum and Strauch 1968), and the same is true for the OSM, which ranges from 50 to 200 m in the model (vs. a maximum of *c*. 70 m; see Unger 1984). These differences occur because we have now integrated into the model data from boreholes that have been drilled over the past 40 years and cover regions for which Unger (1984) had no information.

## Synthesis of stratigraphic and tectonic data

The depth maps indicate areas of variable subsidence during deposition of the OMM, Onc Fm and OSM (Fig. 8). The Braunau Trough was considered to be the deepest part of the OMM basin by previous authors (Unger and Schwarzmeier 1982; Lemcke 1988). Indeed, our model confirms that the Braunau Trough underwent significant subsidence, but the deepest sector during the time of OMM and OBM was the southern area of the Landshut–Neuötting High (as revealed by the steep dipping of the modeled units shown in Fig. 8, and the high thicknesses in this area depicted in Figs. 9 and 10). The Landshut–Neuötting High thus acted not as a 'high' but as a trough in the middle and late Burdigalian.

Phases of erosion have been reported based on outcrop data, drilling results and seismological investigations from the adjacent area of Upper Austria, where "within the Ottnangian every formation begins and ends with a major submarine erosion" (Wagner 1998: 358). Our 3D

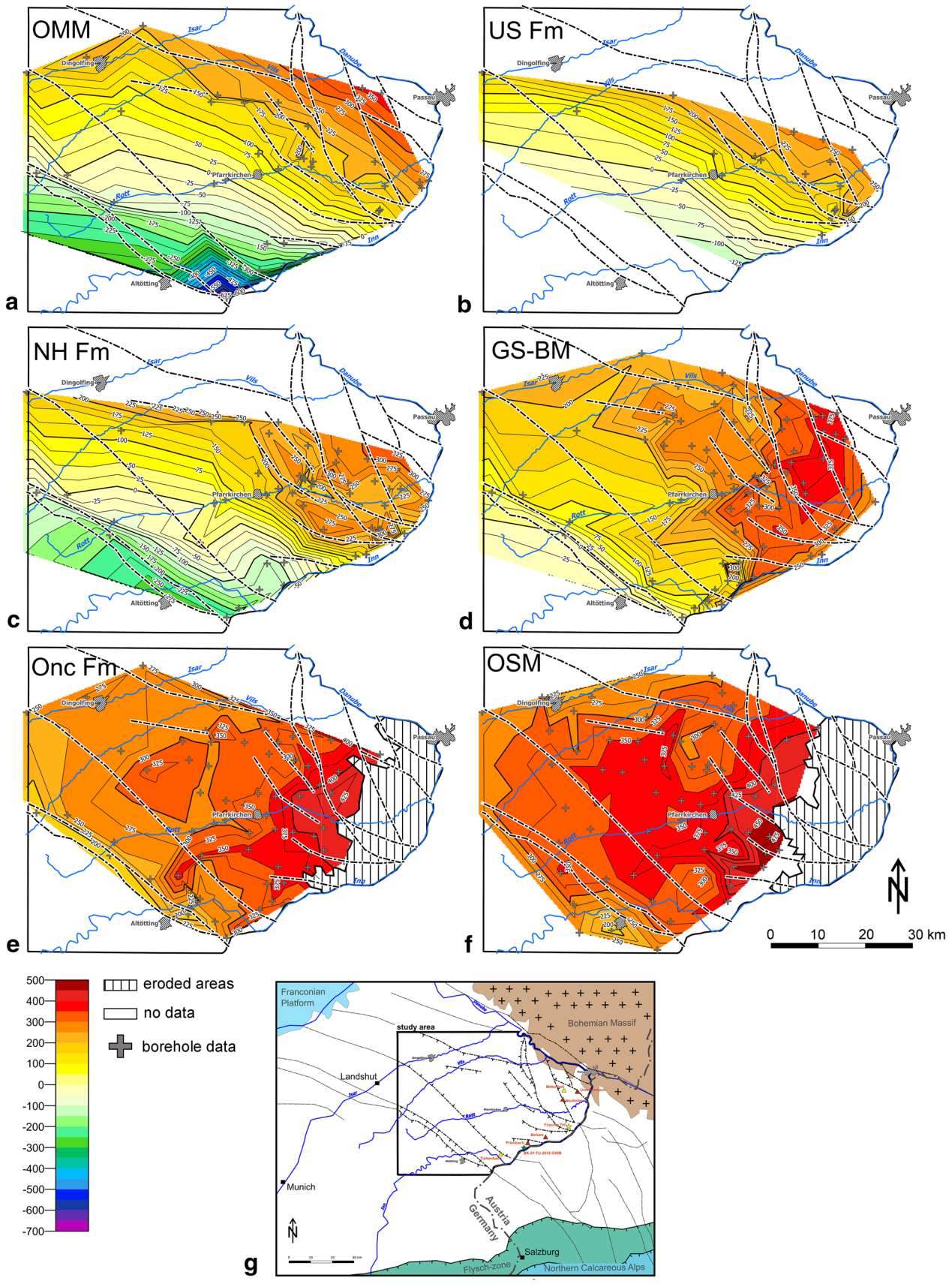
OMM
US Fm
NH Fm
GS-BM
Onc Fm
OSM
a
b
c
d
e
f
Dingolfing
Passau
Pfarrkirchen
Altötting
Isar
Vils
Rott
Inn
Danube
0 10 20 30 km
500
400
300
200
100
0
-100
-200
-300
-400
-500
-600
-700
eroded areas
no data
borehole data
g
Franconian Platform
Bohemian Massif
study area
Landshut
Munich
Austria
Germany
Salzburg
Flysch-zone
Northern Calcareous Alps

◂**Fig. 8** **a–f** Depth maps (m.a.s.l.) for strata bases reconstructed from the 3D model. Crosses indicate boreholes which yielded depth data used for the respective modeled base. Isolines are placed at 50-m intervals. **g** Overview of the study area in the SE German part of the NAFB

geological model indicates a clear phase of erosion solely at the Eggenburgian–Ottnangian boundary, because the US Fm fills a palaeorelief within the Eggenburgian strata (Profiles B–C). It coincides with the distinctive hiatus at the end of the Eggenburgian, which has been recognized in the study area and throughout the Paratethys based on outcrop observations and abrupt changes in benthic foraminifers (Wenger 1987; Kovác et al. 2004; Piller et al. 2007; Pippèrr and Reichenbacher 2009). Combining the results derived from the 3D geological model suggests the following scenario for the deposition of the Ottnangian strata (from old to young, see also Fig. 11).

1. After the end-Eggenburgian erosion period, the US Fm, NH Fm and lower GS-BM accumulated.
2. A faulting event then occurred. It probably caused the cessation of the subsidence of the Braunau Trough. Submarine currents and turbulences may have eroded parts of the GS-BM, but this is difficult to prove because the GS-BM is generally poor in foraminifers. This faulting phase was most probably a supra-regional event, because it is likely that the emergence of brackish facies in the lower GS-BM, evidenced in a core obtained *c*. 150 km west of our study area, can be related to it (drilling site Stockhausen, Pippèrr 2011).
3. The upper GS-BM and lower Onc Fm accumulated.
4. A second faulting event occurred. It affected the main faults bounding the Braunau Trough, which continue into Austria (see Fig. 3a and Wagner 1998). It is thus likely that this faulting phase too was a supra-regional event.
5. The upper Onc FM and OSM accumulated. As the OSM is a fluvial deposit, the Onc Fm/OSM contact may be erosive, but in general it is undisturbed.
6. Post-OSM uplift and tilting of the entire area to the west led to erosion of the OSM (which is now thickest in the west). The same uplift, tilting and subsequent erosion, with the removal of some 500–900 m of OSM deposits, have previously been reported for the Austrian part of the NAFB, adjacent to our study area (Gusterhuber et al. 2012). The prominent uplift was probably related both to the isostatic rebound of the Alps and E-W compression of the Alpine, Carpathian and Dinarides mountain belts (Sissingh 2006; Gusterhuber et al. 2012; Ortner et al. 2015).

## A revised age model for the middle to late Burdigalian in the eastern Molasse Basin

The Eggenburgian–Ottnangian boundary is generally correlated with the global sea-level lowstand Bur3, thereby assigning the basis of the Ottnangian to 18.2 Ma (Krijgsman and Piller 2012; Pippèrr et al. 2018). This assumption is supported by biostratigraphic data derived from the identification of the nannoplankton zones "upper NN3 to lower NN4" in the NH Fm (Martini 1981) and Ottnang Fm (Grunert et al. 2011). NN3 extends from 18.28 to 17.95 Ma (Hilgen et al. 2012). "Upper NN3" thus implies a maximum age of *c*. 18.1 Ma for the NH Fm and Ottnang Fm. NN4 spans the interval from 17.95 to 14.95 Ma (Hilgen et al. 2012). It can thus be assumed that "lower NN4" approximately matches the time window 17.95–16.5 Ma (which encompasses the lower half of the entire NN4 zone). This suggests a minimum age of 16.5 Ma for the NH Fm and Ottnang Fm.

The model indicates that the outcrops Untersimbach (exposing the US Fm) and Neuhofen (exposing the NH Fm), which both have normal polarity, are separated by *c*. 80 m of rocks (Fig. 9c). This casts doubt on the conclusion drawn by Pippèrr et al. (2018) that the normal polarities of Untersimbach and Neuhofen both belong to upper chron C5En (equaling 18.2–18.06 Ma) because this would require a very high accumulation rate for the NH Fm (93.3 cm/ky, see Table 3). Here, we follow Pippèrr et al. (2018) in attributing the normal polarity of the Untersimbach outcrop to upper chron C5En. But we assign the NH Fm documented by the exposure at Neuhofen to the short normal chron C5Dr.1n (Fig. 11). The model also indicates that the NH Fm at Mitterdorf follows only few meters above the NH Fm at Neuhofen (Fig. 10c). As a result, the lower part of the NH Fm at Mitterdorf, which exhibits reverse polarity, is correlated here to C5Dr.1r (and not to C5Dr.2r as proposed in Pippèrr et al. 2018), and the upper part of the NH Fm at Mitterdorf, which we have confirmed to be of normal polarity, is correlated here with C5Dn (Fig. 11). This in turn necessitates correlation of the relatively long interval of normal polarity (18 m) seen in the GS-BM at Beham also with chron C5Dn, and the uppermost segment of reverse polarity at Beham with chron C5Cr (Fig. 11). The next available magnetic data are from the uppermost GS-BM and lowermost Onc Fm at Prienbach; all these samples were of normal polarity. We attribute them to chron C5Cn.3n, because it is the next normal chron (Fig. 11). We do not have polarity data for the remaining lower Onc Fm, but we recorded a reverse polarity from the upper Onc Fm (Fig. 6). Possible chrons for this reverse phase are C5Cn.1r or C5Cn.2r. Assignment to C5Cn.2r would imply an accumulation rate of c. 77 cm/k.y. for the Onc Fm, which we consider too high (see below for discussion of accumulation rates).

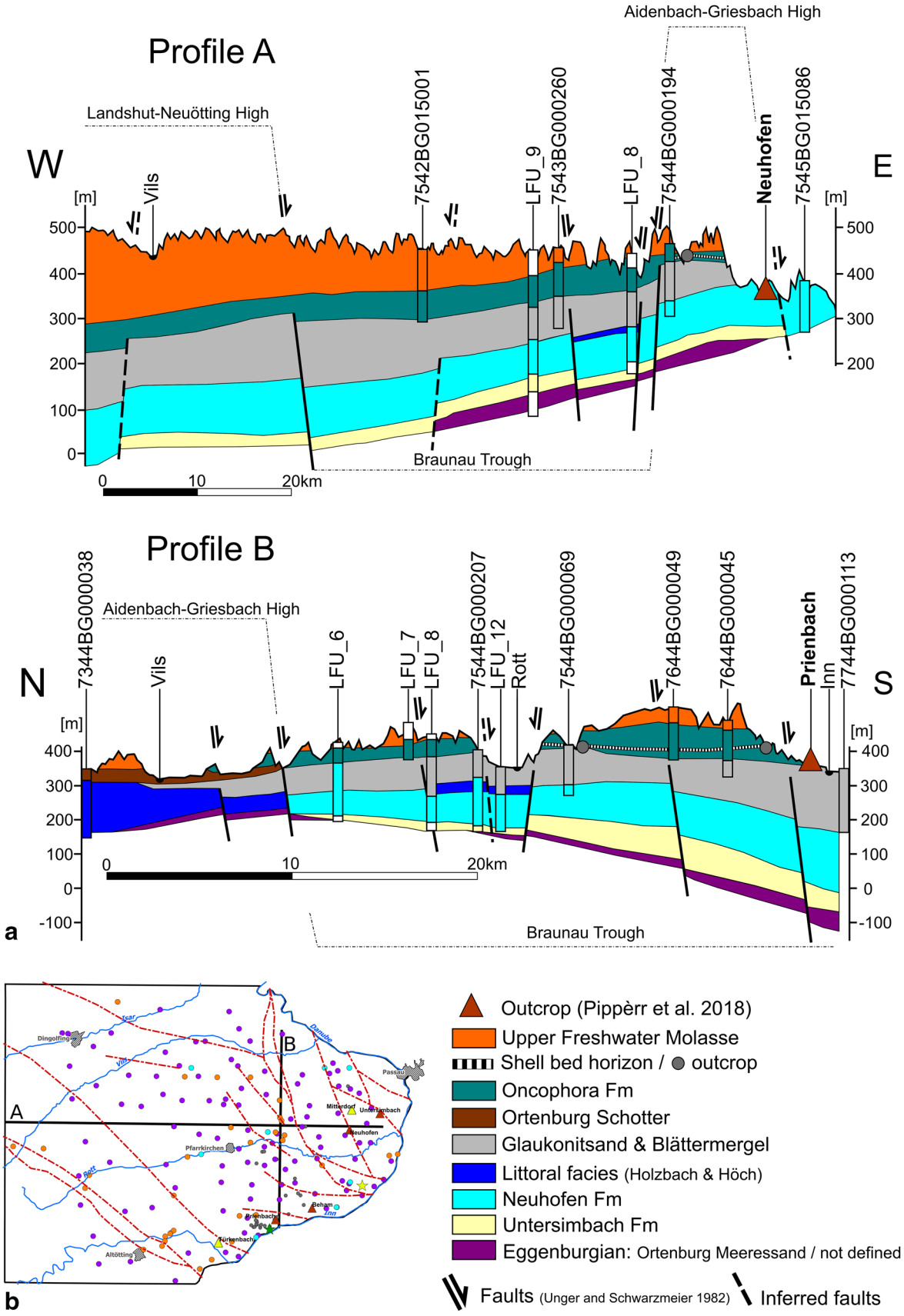
Profile A
Aidenbach-Griesbach High
Landshut-Neuötting High
W
E
[m]
Vils
7542BG015001
LFU_9
7543BG000260
LFU_8
7544BG000194
Neuhofen
7545BG015086
500
400
300
200
100
0
Braunau Trough
0
10
20km
Profile B
N
S
7344BG000038
Aidenbach-Griesbach High
Vils
LFU_6
LFU_7
LFU_8
7544BG000207
LFU_12
Rott
7544BG000069
7644BG000049
7644BG000045
Prienbach
Inn
7744BG000113
400
300
200
100
0
-100
0
10
20km
Braunau Trough
a
A
B
Dingolfing
Isar
Vils
Rott
Donau
Inn
Passau
Mitterdorf
Untersimbach
Neuhofen
Pfarrkirchen
Braunau
Beham
Türkenbach
Altötting
b
Outcrop (Pippèrr et al. 2018)
Upper Freshwater Molasse
Shell bed horizon / outcrop
Oncophora Fm
Ortenburg Schotter
Glaukonitsand & Blättermergel
Littoral facies (Holzbach & Höch)
Neuhofen Fm
Untersimbach Fm
Eggenburgian: Ortenburg Meeressand / not defined
Faults (Unger and Schwarzmeier 1982)
Inferred faults

◂**Fig. 9** **a** Geological cross sections based on the 3D model from west to east (Profile A) and north to south (Profile B). Data on faults and inclination are adapted from Unger (1984) and Unger and Schwarzmeier (1982). Note that the lines at the bases of the Untersimbach Fm and Eggenburgian do not represent their true bases (owing to lack of drilling data). The stratigraphic column of LfU_6 is given according to the original borehole description, but it is likely that the upper part of the borehole (indicated as NH Fm) actually corresponds to the GS-BM. **b** Study area with positions of the profiles A and B (see Fig. 4 for close-up)

Therefore, we correlate the reverse polarity of the upper Onc Fm with chron C5Cn.1r. The resulting accumulation rate (c. 25 cm/k.y.) is in the same range as the rate we calculated for the GS-BM (Table 3) and seems reasonable (see below).

Our revised correlation fits well with reverse polarity data obtained at the outcrop Ottnang-Schanze in Upper Austria by Grunert et al. (2011). Ottnang-Schanze exposes strata that are very similar to those of the NH Fm at the Neuhofen outcrop (Pippèrr 2011; Grunert et al. 2012), and a similar age for both outcrops is likely. In the study by Grunert et al. (2014), the reverse polarity of Ottnang-Schanze is dated to 17.85–17.86 Ma. This is entirely consistent with our age model, as Ottnang-Schanze plots directly beneath the normal polarity of the outcrop Neuhofen (Fig. 11). Further support for this correlation comes from the fact that Ottnang-Schanze represents the lower part of the Ottnang Fm (Grunert et al. 2011).

The new age model is compatible with previous reports of $^{87}Sr/^{86}Sr$ age ranges based on ostracods and otoliths (Janz and Vennemann 2005; Teschner and Reichenbacher 2017). The ostracods analyzed originated from the Neuhofen outcrop, and Janz and Vennemann (2005) reported a mean $^{87}Sr/^{86}Sr$ value of $0.708624 \pm 0.000010$ for them. The dated otoliths were collected from the NH Fm exposed at Mitterdorf and provided a mean $^{87}Sr/^{86}Sr$ value of $0.708645 \pm 0.000012$ (Teschner and Reichenbacher 2017). Using the global marine Sr isotope curve (LOWESS 5 fit) of McArthur et al. (2012), the $^{87}Sr/^{86}Sr$ values cited above imply depositional age ranges of 17.1–17.7 Ma ($17.4 \pm 0.3$) Ma (Neuhofen) and 16.8–17.4 ($17.1 \pm 0.3$) Ma (Mitterdorf), respectively (see Teschner and Reichenbacher 2017: fig. 3). In the case of Neuhofen, the maximum value (17.7 Ma) of the Sr age range conforms to our new age model, while in the case of Mitterdorf the maximum value (17.4 Ma) is about 0.1 Ma too young. Although these Sr age ranges indicate surprisingly "young" age ranges, we consider them to be reliable, because the NAFB was an open marine environment at the time of the NH Fm, and was assuredly connected to the Mediterranean Sea (Burdigalian Seaway, see also Janz and Vennemann 2005). It is also conceivable that the global marine Sr isotope curve is not entirely accurate at the time window considered here (oral communication from A. Rocholl, Potsdam).

In this context, a comment on the $^{87}Sr/^{86}Sr$ age range of 18.1–17.5 Ma ($17.8 \pm 0.3$) provided by Pippèrr et al. (2007) is called for, because this datum has often been used as an age constraint for the basis of the middle Ottnangian (e.g., Reichenbacher et al. 2013; Grunert et al. 2014; Pippèrr et al. 2018). Table 4 shows the individual measurements reported in Pippèrr et al. (2007), which were obtained for the otoliths of a nektonic fish (a sciaenid) and a benthonic fish (a congrid). The authors then used the sample mean to calculate the age on the basis of the global marine Sr curve of Howarth and McArthur (2003). According to the revised curve subsequently reported by McArthur et al. (2012), however, that average value equates to a slightly younger age range, i.e., 17.8–17.2 ($17.5 \pm 0.3$) Ma. This revised age range fits well with our new age model, as the basis of the GS-BM (= basis 'middle Ottnangian') is at *c*. 17.45 Ma (Fig. 11).

## Notes on accumulation rates

Accumulation rates are calculated by dividing the preserved strata thickness by the time available for their deposition (Schlunegger et al. 1997; Kempf et al. 1999; Kirscher et al. 2016). Previously reported accumulation rates for Molasse deposits are highly variable, ranging from < 10 to > 100 cm/k.y., with the lowest values in distal areas and the highest in deep basins or near the Alps (e.g., Sant et al. 2017; van der Boon et al. 2018). Previously reported values for OMM sedimentation rates are between 20 and 30 cm/k.y. (Kempf et al. 1999; Jost et al. 2006), but these values were calculated for the western part of the NAFB, where the basin was shallower than in the eastern part (Pippèrr 2011). Accumulation rates for the Onc Fm have not yet been calculated.

Here, we calculated accumulation rates (cm/k.y.) for the Braunau Trough on the basis of the maximum strata thicknesses derived from the 3D geological model and applying the age models of our study and Pippèrr et al. (2018). Based on the latter age model, accumulation rates would be *c*. 93 cm/k.y. for the NH Fm, and then would decrease to *c*. 50 cm/k.y. for the GS-BM and to *c*. 14 cm/k.y. for the Onc Fm (Table 3). When our new age model is applied, the NH Fm reveals an accumulation rate of *c*. 43 cm/k.y., and the value obtained for the GS-BM and the Onc Fm is 25 cm/k.y. in each case. In both age models, the highest values derive from the NH Fm, which is plausible because the Braunau Trough experienced greater subsidence at the corresponding time than later (see above and Fig. 8). The decrease in the accumulation rate of the GS-BM, seen in both models, is also reasonable, because a faulting phase occurred during the GS-BM (see above and Fig. 11). But only in our age model is the estimated accumulation rate for the subsequent deposits of the Onc Fm comparable to that for the GS-BM,

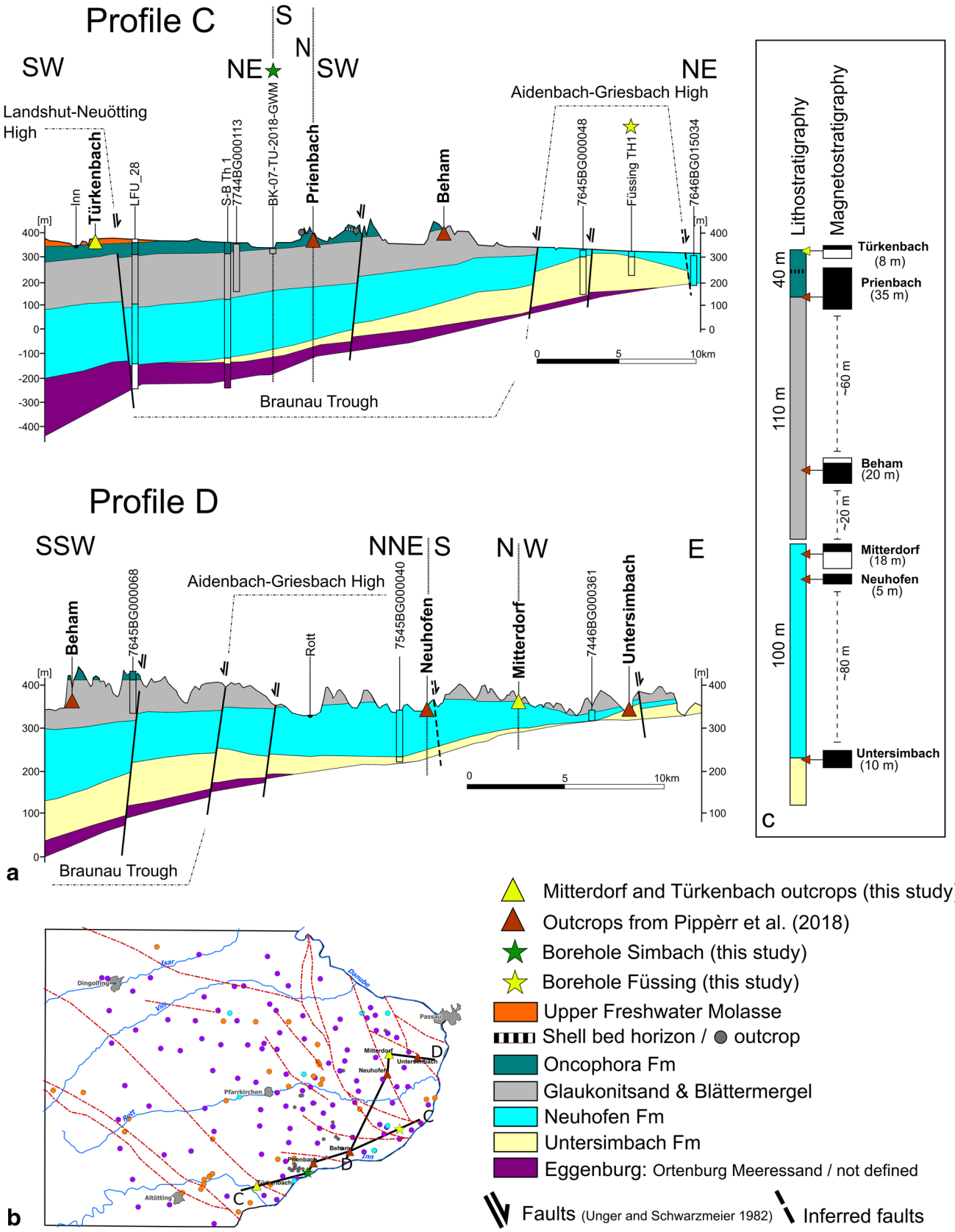
Profile C
SW
S
N
NE
SW
NE
Landshut-Neuötting High
Aidenbach-Griesbach High
Inn
Türkenbach
LFU_28
S-B Th 1
7744BG000113
BK-07-TU-2018-GWM
Prienbach
Beham
7645BG000048
Füssing TH1
7646BG015034
[m]
400
300
200
100
0
-100
-200
-300
-400
0
5
10km
Braunau Trough
Profile D
SSW
NNE
S
N
W
E
Beham
7645BG000068
Aidenbach-Griesbach High
Rott
7545BG000040
Neuhofen
Mitterdorf
7446BG000361
Untersimbach
Braunau Trough
a
Lithostratigraphy
Magnetostratigraphy
40 m
110 m
100 m
Türkenbach
(8 m)
Prienbach
(35 m)
~60 m
Beham
(20 m)
~20 m
Mitterdorf
(18 m)
Neuhofen
(5 m)
~80 m
Untersimbach
(10 m)
c
b
Dingolfing
Isar
Donau
Vils
Passau
Mitterdorf
Untersimbach
Neuhofen
Pfarrkirchen
Rott
Inn
Beham
Prienbach
Türkenbach
Altötting
A
B
C
D
Mitterdorf and Türkenbach outcrops (this study)
Outcrops from Pippèrr et al. (2018)
Borehole Simbach (this study)
Borehole Füssing (this study)
Upper Freshwater Molasse
Shell bed horizon / outcrop
Oncophora Fm
Glaukonitsand & Blättermergel
Neuhofen Fm
Untersimbach Fm
Eggenburg: Ortenburg Meeressand / not defined
Faults (Unger and Schwarzmeier 1982)
Inferred faults

◂**Fig. 10** **a** Geological cross sections based on the 3D model depicting the intersection of outcrops with the model. Data on faults and inclination are adapted from Unger (1984) and Unger and Schwarzmeier (1982). **b** Study area with positions of the profiles C and D (see Fig. 4 for close-up). **c** Column indicating thicknesses of strata and positions of outcrops, as derived from the model, and polarity data of outcrops according to Pippèrr et al. (2018) and this study (Türkenbach)

while the model of Pippèrr et al. (2018) yields a significantly lower value (Table 3). This can be interpreted in terms of our model, because the Onc Fm was deposited close to a deltaic system (Schlickum and Strauch 1968; Haas 1987) and its sedimentation rate was probably similar to that of the GS-BM. Further support comes from empirical evidence which suggests that as long as accommodation space and subsidence remain stable within a given area—which is the case for the GS-BM and Onc Fm according to our model—accumulation rates should be relatively constant through time (Kempf and Pross 2005; Sant et al. 2017).

## Supra-regional correlation

The correlation between the eastern Molasse of the south German sector of the NAFB (represented by our study area) and the Molasse of upper Austria is well established (Rupp et al. 2008; Grunert et al. 2011; Pippèrr et al. 2018; see Fig. 11). It thus can be assumed that our new age model also applies for the strata of the upper Austrian Molasse Basin; however, future work will be necessary to corroborate this. That strata considered as "lower Ottnangian" may be younger than previously thought even in other parts of the Austrian Molasse Basin has been demonstrated in Lower Austria. Roetzel et al. (2014) recorded a $^{40}Ar/^{39}Ar$ age of $17.23 \pm 0.18$ Ma for an ash layer above the Zellerndorf Fm, which had until then been considered as "lower Ottnangian" (Grunert et al. 2010). Roetzel et al. (2014) concluded on the basis of their new age datum that the Zellerndorf Fm relates to the Ottnangian or early Karpatian. This supports our inference that what has hitherto been regarded as "lower Ottnangian" actually represents almost the entire Ottnangian stage in its current definition.

There is also an established correlation of the OMM and OBM between the eastern and western Molasse of the south German portion of the NAFB (Heckeberg et al. 2010; Pippèrr et al. 2016; Pippèrr and Reichenbacher 2017). However, this correlation is subject to uncertainties, mainly because the lithofacies and benthic foraminiferal assemblages differ considerably between the eastern and western Molasse, and absolute age constraints are scarce (see discussions in Tipper

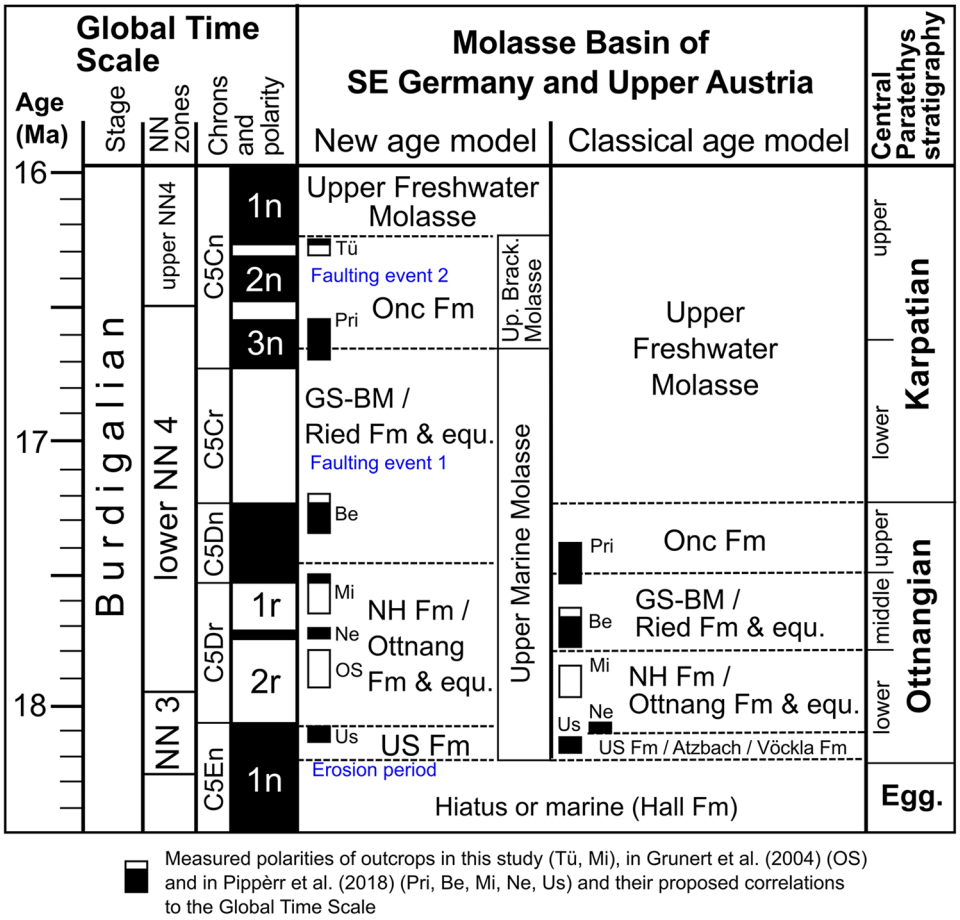


**Fig. 11** Chart depicting the new age model derived in our study in comparison to the classical age models according to Pippèrr et al. (2018) for the SE German Molasse Basin and Rupp et al. (2008) for the Upper Austrian Molasse Basin. Global Time Scale, chrons, polarities, and correlation of Central Paratethys stages are taken from Hilgen et al. (2012), while the base of the Ottnangian is adapted from Pippèrr et al. (2018). Abbreviations for outcrop names: *Tü* Türkenbach, *Pri* Prienbach, *Be* Beham, *Mi* Mitterdorf, *Ne* Neuhofen, *OS* Ottnang Schanze, *Us* Untersimbach. Abbreviations of lithostratigraphic units: *Onc Fm* Oncophora Fm, *GS-BM* Glimmersand & Blättermergel, *NH Fm* Neuhofen Fm, *US Fm* Untersimbach Fm, *equ.* equivalent strata without formal names

**Table 3** Sediment accumulation rates (cm/k.y.) in the Braunau Trough when different age models are applied

| Age model/lithostratigraphic units | NH Fm<br>280 m | GS-BM<br>200 m | OPH Fm<br>100 m |
|---|---|---|---|
| This study | 18.1–17.45 Ma<br>43.1 cm/k.y. | 17.45–16.65 Ma<br>25.0 cm/k.y. | 16.65–16.25 Ma<br>25.0 cm/k.y. |
| Pippèrr et al. (2018) | 18.1–17.8 Ma<br>93.3 cm/ky | 17.8–*c*. 17.4 Ma<br>50.0 cm/k.y. | 17.4–*c*. 16.72 Ma<br>14.3 cm/k.y. |
| Subsidence | ++ | + | + |

Maximal thicknesses (m) of strata and estimation of subsidence are based on the 3D geological model

**Table 4** $^{87}Sr/^{86}Sr$ values reported by Pippèrr et al. (2007) and their new age interpretation using the global marine Sr curve of McArthur et al. (2012)

| Data from Pippèrr et al. (2007: table 4) | | | Revised age |
|---|---|---|---|
| Sample | Values | Error | |
| Sciaenid L1 | 0.708595 | 09 | |
| Sciaenid L2 | 0.708614 | 14 | |
| Sciaenid L4-1 | 0.708615 | 11 | |
| Sciaenid L4-2 | 0.708599 | 14 | |
| Congrid L3a | 0.708633 | 08 | |
| Congrid L3b | 0.708642 | 18 | |
| Mean all | 0.708615 | ±36 | 17.5 ± 0.3 |

et al. 2003; Pippèrr et al. 2007; Reichenbacher et al. 2013; Frieling et al. 2009; Sant et al. 2017). Again, further work will be needed to confirm or refute this correlation.

In the NAFB and Central Paratethys, the major disruptive tectonic activities associated with erosion have been recorded for the Karpatian stage (Gusterhuber et al. 2012; Reichenbacher et al. 2013). Gusterhuber et al. (2012) found that these resulted in a slight tilting of the NAFB to the west (slope of about 0.5%). Given our new age model, it is very likely that the tectonic events discerned in our study are both related to the large-scale tectonic movements that affected the NAFB during the Karpatian stage.

## Conclusion

The high-resolution 3D reconstruction of the Burdigalian sediments in the southeast German part of the NAFB presented here provides a detailed picture of the geological conditions during this interval. Completely new insights pertaining to (1) the isochrony of strata, (2) subsidence, and (3) synsedimentary tectonics have been obtained. The two faulting phases recognized probably correspond to a major tectonic event in the Karpatian that affected the entire NAFB (Gusterhuber et al. 2012).

A further important result is a revised age model for the middle and upper Burdigalian strata in the southeast German part of the NAFB and Upper Austria. Compared to previous studies, it indicates substantially—up to 0.8 Ma—younger ages for the OMM and Onc Fm. Approximate temporal ranges for the studied strata are: Onc Fm 16.25–16.65 Ma, GS-BM 16.65–17.45 Ma, NH Fm 17.45–18.1 Ma, and US Fm 18.1–18.2 Ma. The new age model is compatible with previously reported Sr-age ranges from the Neuhofen Fm (Janz and Vennemann 2005; Teschner and Reichenbacher 2017).

We conclude that, in the southeast German and Upper Austrian sector of the NAFB, the classical "lower Ottnangian" represents the entire Ottnangian in its current definition. Whether or not the upper boundary of the Ottnangian stage must be revised to integrate the "middle" and "upper Ottnangian" that, according to our new age model, now lie outside the Ottnangian stage remains a question for future work.

**Acknowledgements** For providing access to drilling sites and well samples, we are grateful to the engineering companies Müller and Hereth GmbH (Simbach, Germany), with special thanks to Michael Schmid and Dr. Marcus Scholz, and to Piewak and Partner GmbH (Füssing, Germany), with special thanks to Manfred Piewak. We thank Dr. Martina Pippèrr (LMU Munich, Germany), Dr. Alexander Rocholl (GFZ Potsdam, Germany) and Prof. Dr. Valerian Bachtadse (LMU Munich) for precious comments and discussion. For discussions on 3D modeling and stratigraphic issues, we thank Dr. Robert Pamer (LfU, Augsburg, Germany), Dr. Kai Zosseder (TU Munich, Germany), Ulrich Haas and Martin Herz (both LfU, Hof, Germany). We are grateful to Johannes Großmann (LfU, Augsburg, Germany) for providing new results on the Wolfach Fault. We are indebted to Marija Ivanovic (LfU, Augsburg, Germany) for her invaluable assistance with sample processing and microfossil picking of the Füssing -TH 1 samples. For help in identifying fossils, we thank Inda Brinkmann (Lund University, Sweden), Dr. Werner Schwarzhans (Hamburg, Germany) and Dr. Mathias Harzhauser (Natural History Museum, Vienna, Austria). The manuscript benefited greatly from the constructive comments of the reviewers Prof. Dr. P. Grunert (Univ. Köln, Germany) and Dr. Ch. Rupp (GBA Wien, Austria), and from the critical reading of Dr. P. Hardy (Düsseldorf, Germany). Finally, we acknowledge the students and lecturers involved in the Master's program in Geobiology and Paleobiology at LMU, who provided a stimulating environment for this work.

## References

Abdul-Aziz H, Böhme M, Rocholl A, Prieto J, Wijbrans JR, Bachtadse V, Ulbig A (2010) Integrated stratigraphy and $^{40}Ar/^{39}Ar$

chronology of the Early to Middle Miocene Upper Freshwater Molasse in western Bavaria (Germany). Int J Earth Sci 99:1859–1886

Allen PA, Mange-Rajetzky M, Matter A, Homewood P (1985) Dynamic paleogeography of the open Burdigalian seaway, Swiss Molasse basin. Eclogae Geol Helv 78:351–386

Bachmann GH, Müller M (1992) Sedimentary and structural evolution of the German Molasse Basin. Eclogae Geol Helv 85:519–530

Berger J-P et al (2005) Eocene-Pliocene time scale and stratigraphy of the Upper Rhine Graben (URG) and the Swiss Molasse Basin (SMB). Int J Earth Sci 94:711–731. https://doi.org/10.1007/s00531-005-0479-y

Binder H (2004) Terrestrial, freshwater and brachyhaline Gastropoda from the Lower Miocene deposits of Oberdorf (Styria, Austria). Annalen des Naturhistorischen Museums in Wien Serie A für Mineralogie und Petrographie, Geologie und Paläontologie, Anthropologie und Prähistorie 105 A:189–229

Böhme M (2003) The Miocene Climatic Optimum: evidence from ectothermic vertebrates of Central Europe. Palaeogeogr Palaeoclimatol Palaeoecol 195:389–401. https://doi.org/10.1016/s0031-0182(03)00367-5

Brinkmann I, Pippèrr M, Reichenbacher B (2019) A new well-preserved ostracod fauna from the middle Burdigalian (lower Miocene) of the North Alpine Foreland Basin. Geobios. https://doi.org/10.1016/j.geobios.2019.07.005

Cicha I, Rögl F, Rupp C, Ctyroka J (1998) Oligocene-Miocene foraminifera of the Central Paratethys. Abhandlungen der Senckenbergischen Naturforschenden Gesellschaft 549:1–325

Čtyroký P, Kantorová V, Ondrejíčková A, Strauch F, Vass D (1973) Faziostratotypen der *Rzehakia* (*Oncophora*) Formation. In: Papp A, Rögl F, Seneš J (eds) Chronostratigraphie und Neostratotypen Miozän der zentralen Paratethys, vol III. $M_2$ Ottnangien Die Innviertler, Salgótarjáner. Bántapusztaer Schichtengruppe und die Rzehakia Formation. Slowakische Akademie der Wissenschaften, Bratislava, pp 244–265

Diepolder GW et al (2011) Geowissenschaftliche Landesaufnahme in der Planungsregion 12 Donau-Wald. Bayerisches Landesamt für Umwelt, Augsburg

Doppler G, Heissig K, Reichenbacher B (2005) Die Gliederung des Tertiärs im süddeutschen Molassebecken. Newsl Stratigr 41:359–375. https://doi.org/10.1127/0078-0421/2005/0041-0359

Frieling D, Aehnelt M, Scholz H, Reichenbacher B (2009) Sequence stratigraphy of an alluvial fan-delta in the Upper Marine Molasse (Pfänder area, Late Burdigalian, Miocene). Z Dtsch Ges Geowiss 160:333–357. https://doi.org/10.1127/1860-1804/2009/0160-0333

Garefalakis P, Schlunegger F (2019) Deciphering tectonic, eustatic and surface controls on the 20 Ma-old Burdigalian transgression recorded in the Upper Marine Molasse in Switzerland. Solid Earth Discuss. https://doi.org/10.5194/se-2019-27 **(in review)**

Goldbrunner JE, Vasvári V, Kolb A (2001) Die Bohrung Simbach-Braunau Thermal 1 Technischer Ablauf und hydrogeologische Ergebnisse. Geol Bavarica 106:59–79

Grimm WD (1963) Der Schillhorizont in der ostniederbayerischen Süßbrackwassermolasse und seine bergbauliche Gewinnung. Geol Mitt 3:221–252

Grunert P, Soliman A, Harzhauser M, Müllegger S, Piller WE, Roetzel R, Rögl F (2010) Upwelling conditions in the Early Miocene Central Paratethys Sea. Geol Carpath 61:129–145. https://doi.org/10.2478/v10096-010-0006-3

Grunert P, Soliman A, Ćorić S, Scholger R, Harzhauser M, Piller WE (2011) Stratigraphic re-evaluation of the stratotype for the regional Ottnangian stage (Central Paratethys, middle Burdigalian). Newsl Stratigr 44:1–16. https://doi.org/10.1127/0078-0421/2010/0001

Grunert P, Soliman A, Ćorić S, Roetzel R, Harzhauser M, Piller WE (2012) Facies development along the tide-influenced shelf of the Burdigalian Seaway: an example from the Ottnangian stratotype (Early Miocene, middle Burdigalian). Mar Micropaleontol 84–85:14–36. https://doi.org/10.1016/j.marmicro.2011.11.004

Grunert P, Tzanova A, Harzhauser M, Piller WE (2014) Mid-Burdigalian Paratethyan alkenone record reveals link between orbital forcing, Antarctic ice-sheet dynamics and European climate at the verge to Miocene Climate Optimum. Global Planet Change 123:36–43. https://doi.org/10.1016/j.gloplacha.2014.10.011

Grunert P, Auer G, Harzhauser M, Piller WE (2015) Stratigraphic constraints for the upper Oligocene to lower Miocene Puchkirchen Group (North Alpine Foreland Basin, Central Paratethys). Newsl Stratigr 48:111–133. https://doi.org/10.1127/nos/2014/0056

Gusterhuber J, Dunkl I, Hinsch R, Linzer H-G, Sachsenhofer R (2012) Neogene uplift and erosion in the Alpine foreland basin (upper Austria and Salzburg). Geol Carpath 63:295–305

Haas J (1987) Das Ortenburger Schotter-Delta in der Süßbrackwassermolasse von Ostniederbayern - geologische, sedimentpetrographische und terrestrisch-photogrammetrische Untersuchungen. Dissertation, Ludwig-Maximilians-Universität

Hagn H (1953) Paläontologische Untersuchungen am Bohrgut der Bohrungen Ortenburg CF 1001, 1002 und 1003 in Niederbayern. Zeitschrift der Deutschen Geologischen Gesellschaft 105:324–358

Hagn H, Malz H, Martini E, Weiss W, Witt W (1981) Exkursion G: Miozäne Vorland-Molasse Niederbayerns und Kreide von Regensburg. Geol Bavarica 82:272–278

Harzhauser M, Piller WE (2007) Benchmark data of a changing sea—palaeogeography, palaeobiogeography and events in the Central Paratethys during the Miocene. Paleogeogr Paleoclimatol Paleoecol 253:8–31. https://doi.org/10.1016/j.palaeo.2007.03.031

Heckeberg N, Pippèrr M, Lauchli B, Heimann FUM, Reichenbacher B (2010) The Upper Marine Molasse (Burdigalian, Ottnangian) in Southwest Germany—facies interpretation and a new lithostratigraphic terminology. Z Dtsch Ges Geowiss 161:285–302. https://doi.org/10.1127/1860-1804/2010/0161-0285

Hilgen F, Lourens LJ, Van Dam JA (2012) The Neogene Period. In: Gradstein FM, Ogg JG, Schmitz MD, Ogg GM (eds) The Geologic Time Scale 2012, vol 1. Elsevier, Amsterdam, pp 923–978

Hofmann GW (1967) Untersuchungen an der Gattung *Bolivina* (Foraminifera) im Oligozan und Miozän der ostbayerischen Molasse. Geol Bavarica 57:121–204

Howarth RJ, McArthur JM (2003) SIS Look-up table, Version 4: 08/03. Received by personal communication

Janssen R et al (2018) Das Tertiär in der Stratigraphischen Tabelle von Deutschland 2016. Z Dtsch Ges Geowiss 169:267–294. https://doi.org/10.1127/zdgg/2018/0152

Janz H, Vennemann TW (2005) Isotopic composition (O, C, Sr, and Nd) and trace element ratios (Sr/Ca, Mg/Ca) of Miocene marine and brackish ostracods from North Alpine Foreland deposits (Germany and Austria) as indicators for palaeoclimate. Palaeogeogr Palaeoclimatol Palaeoecol 225:216–247. https://doi.org/10.1016/j.palaeo.2005.06.012

Jost J, Kälin D, Schulz-Mirbach T, Reichenbacher B (2006) Late Early Miocene lake deposits near Mauensee, central Switzerland: fish fauna (otoliths, teeth), accompanying biota and palaeoecology. Eclogae Geol Helv 99:309–326. https://doi.org/10.1007/s00015-006-1198-5

Kälin D, Kempf O (2009) High-resolution stratigraphy from the continental record of the Middle Miocene Northern Alpine Foreland Basin of Switzerland. Neues Jahrbuch für Geologie und Paläontologie Abhandlungen 254:177–235. https://doi.org/10.1127/0077-7749/2009/0010

Kempf O, Pross J (2005) The lower marine to lower freshwater Molasse transition in the northern Alpine foreland basin (Oligocene; central Switzerland–south Germany): age and geodynamic implications. Int J Earth Sci 94:160–171. https://doi.org/10.1007/s00531-004-0437-0

Kempf O, Matter A, Burbank DW, Mange M (1999) Depositional and structural evolution of a foreland basin margin in a magnetostratigraphic framework: the eastern Swiss Molasse Basin. Int J Earth Sci 88:253–275. https://doi.org/10.1007/s005310050263

Kirscher U, Prieto J, Bachtadse V, Abdul Aziz H, Doppler G, Hagmaier M, Böhme M (2016) A biochronologic tie-point for the base of the Tortonian stage in European terrestrial settings: magnetostratigraphy of the topmost Upper Freshwater Molasse sediments of the North Alpine Foreland Basin in Bavaria (Germany). Newsl Stratigr 49:445–467. https://doi.org/10.1127/nos/2016/0288

Kirschvink JL (1980) The least-squares line and plane and the analysis of Paleomagnetic data. Geophys J R Astron Soc 62:699–718. https://doi.org/10.1111/j.1365-246X.1980.tb02601.x

Knipscheer HCG (1952) Die Gliederung der ungefalteten Molasse im östlichen Teil Bayerns auf Grund mikropaläontologischer Untersuchungen. Geol Bavarica 14:48–67

Kováč M, Barath I, Harzhauser M, Hlavaty I, Hudackova N (2004) Miocene depositional systems and sequence stratigraphy of the Vienna Basin. Courier Forschungsinstitut Senckenberg 246:187–212

Kowalke T, Reichenbacher B (2005) Early Miocene (Ottnangian) Mollusca of the Western Paratethys—ontogenetic strategies and palaeo-environments. Geobios 38:609–635

Koymans MR, Langereis CG, Pastor-Galán D, van Hinsbergen DJ (2016) Paleomagnetism.org: an online multi-platform open source environment for paleomagnetic data analysis. Comput Geosci 93:127–137. https://doi.org/10.1016/j.cageo.2016.05.007

Krijgsman W, Piller W (2012) Central and Eastern Paratethys. In: Gradstein FM, Ogg JG, Schmitz MD, Ogg GM (eds) The Geologic Time Scale 2012, vol 1. Elsevier, Amsterdam, pp 935–937

Kuhlemann J, Kempf O (2002) Post-Eocene evolution of the North Alpine Foreland Basin and its response to Alpine tectonics. Sediment Geol 152:45–78. https://doi.org/10.1016/s0037-0738(01)00285-8

Lemcke K (1973) Zur nachpermischen Geschichte des nördlichen Alpenvorlandes. Geol Bavarica 69:5–48

Lemcke K (1988) Geologie von Bayern I: Das bayerische Alpenvorland vor der Eiszeit—Erdgeschichte, Bau. Bodenschätze. Schweizerbart, Stuttgart

Martini E (1981) Nannoplankton in der Ober-Kreide, im Alttertiär und im tieferen Jungtertiär von Süddeutschland und dem angrenzenden Österreich. Geol Bavarica 82:345–356

Mayr M (1957) Geologische Untersuchungen in der ungefalteten Molasse im Bereich des unteren Inn: positionsblätter Simbach a. Inn 653 und Julbach 652 Ostteil. Beihefte des Geologischen Jahrbuches 26:309–370

McArthur JM, Howarth RJ, Shields GA (2012) Strontium isotope stratigraphy. In: Gradstein FM, Ogg JG, Schmitz MD, Ogg GM (eds) The Geologic Time Scale. Elsevier, Amsterdam, pp 127–144

McFadden P, McElhinny M (1988) The combined analysis of remagnetization circles and direct observations in palaeomagnetism. Earth Planet Sci Lett 87:161–172

Mullender TAT, Frederichs T, Hilgenfeldt C, de Groot LV, Fabian K, Dekkers MJ (2016) Automated paleomagnetic and rock magnetic data acquisition with an in-line horizontal "2G" system. Geochem Geophys Geosyst 17:3546–3559

Oertli HJ (1956) Ostrakoden aus der oligozänen und miozänen Molasse der Schweiz. Dissertation, University Bern

Olsson RK, Hemleben C, Coxall HK, Wade BS (2018) Taxonomy, biostratigraphy, and phylogeny of Oligocene *Ciperoella* n. gen. In: Wade B, K. Olsson R, Pearson P, Huber B, Berggren W (eds) Atlas of Oligocene Planktonic Foraminifera, vol 46. Cushman Foundation for Foraminiferal Research, Lawrence, pp 215–230

Ortner H, Aichholzer S, Zerlauth M, Pilser R, Fügenschuh B (2015) Geometry, amount, and sequence of thrusting in the Subalpine Molasse of western Austria and southern Germany, European Alps. Tectonics 34:1–30. https://doi.org/10.1002/2014tc003550

Palzer-Khomenko M, Wagreich M, Knierzinger W, Meszar M, Gier S, Kallanxhi M-E, Soliman A (2018) A calcite crisis unravelling Early Miocene (Ottnangian) stratigraphy in the North Alpine-Carpathian Foreland Basin: a litho-and chemostratigraphic marker for the Rzehakia Lake System. Geol Carpath 69:315–334

Pearson PN, Wade BS, Huber BT (2018) Taxonomy, biostratigraphy, and phylogeny of Oligocene Globigerinitidae (*Dipsidripella*, *Globigerinita*, and *Tenuitella*). In: Wade B, K. Olsson R, Pearson P, Huber B, Berggren W (eds) Atlas of Oligocene Planktonic Foraminifera, vol 46. Cushman Foundation for Foraminiferal Research, Lawrence, pp 429–458

Pfleiderer S et al (2016) GeoMol – Geologische 3D-Modellierung des österreichischen Molassebeckens und Anwendungen in der Hydrogeologie und Geothermie im Grenzgebiet von Oberösterreich und Bayern. Abhandlungen der Geologischen Bundesanstalt 70:3–88

Piller WE, Harzhauser M, Mandic O (2007) Miocene Central Paratethys stratigraphy—current status and future directions. Stratigraphy 4:151–168

Pippèrr M (2011) Characterisation of Ottnangian (middle Burdigalian) palaeoenvironments in the North Alpine Foreland Basin using benthic foraminifera—a review of the Upper Marine Molasse of southern Germany. Mar Micropaleontol 79:80–99. https://doi.org/10.1016/j.marmicro.2011.02.002

Pippèrr M, Reichenbacher B (2009) Biostratigraphy and paleoecology of benthic foraminifera from the Eggenburgian "Ortenburger Meeressande" of southeastern Germany (Early Miocene, Paratethys). Neues Jahrbuch für Geologie und Paläontologie Abhandlungen 254:41–61. https://doi.org/10.1127/0077-7749/2009/0003

Pippèrr M, Reichenbacher B (2010) Foraminifera from the borehole Altdorf (SE Germany): proxies for Ottnangian (early Miocene) palaeoenvironments of the Central Paratethys. Palaeogeogr Palaeoclimatol Palaeoecol 289:62–80. https://doi.org/10.1016/j.palaeo.2010.02.009

Pippèrr M, Reichenbacher B (2017) Late Early Miocene palaeoenvironmental changes in the North Alpine Foreland Basin. Palaeogeogr Palaeoclimatol Palaeoecol 468:485–502. https://doi.org/10.1016/j.palaeo.2017.01.002

Pippèrr M, Reichenbacher B, Witt W, Rocholl A (2007) The middle and Upper Ottnangian of the Simssee area (SE Germany): micropalaeontology, biostratigraphy and chronostratigraphy. Neues Jahrbuch für Geologie und Paläontologie Abhandlungen 245:353–378. https://doi.org/10.1127/0077-7749/2007/0245-0353

Pippèrr M, Reichenbacher B, Doppler G, Hagmaier M, Jung D (2016) The northern coast of the Ottnangian (middle Burdigalian, early Miocene) Molasse Sea in Germany: sediments, foraminiferal assemblages and biostratigraphy. Int J Earth Sci 105:1055–1085. https://doi.org/10.1007/s00531-015-1224-9

Pippèrr M, Reichenbacher B, Kirscher U, Sant K, Hanebeck H (2018) The middle Burdigalian in the North Alpine Foreland Basin (Bavaria, SE Germany)—a lithostratigraphic, biostratigraphic and magnetostratigraphic re-evaluation. Newsl Stratigr 51:285–309. https://doi.org/10.1127/nos/2017/0403

Prieto J, Böhme M, Maurer H, Heissig K, Abdul Aziz H (2009) Sedimentology, biostratigraphy and environments of the Untere Fluviatile Serie (Lower and Middle Miocene) in the central part of the North Alpine Foreland Basin—implications for basin evolution. Int J Earth Sci 98:1767–1791

Reichenbacher B (1993) Mikrofaunen, Paläogeographie und Biostratigraphie der miozänen Brack- und Süßwassermolasse

in der westlichen Paratethys unter besonderer Berücksichtigung der Fisch-Otolithen. Senckenb Lethaea 73:277–374

Reichenbacher B et al (2013) A new magnetostratigraphic framework for the Lower Miocene (Burdigalian/Ottnangian, Karpatian) in the North Alpine Foreland Basin. Swiss J Geosci 106:309–334. https://doi.org/10.1007/s00015-013-0142-8

Rocholl A, Schaltegger U, Gilg HA, Wijbrans J, Böhme M (2018) The age of volcanic tuffs from the Upper Freshwater Molasse (North Alpine Foreland Basin) and their possible use for tephrostratigraphic correlations across Europe for the Middle Miocene. Int J Earth Sci 107:387–407

Roetzel R, Ćorić S, Galović I, Rögl F (2006) Early Miocene (Ottnangian) coastal upwelling conditions along the southeastern scarp of the Bohemian Massif (Parisdorf, Lower Austria, Central Paratethys). Beiträge zur Paläontologie (Wien) 30:387–413

Roetzel R et al (2014) Lower Miocene (upper Burdigalian, Karpatian) volcanic ash-fall at the south-eastern margin of the Bohemian Massif in Austria—new evidence from 40Ar/39Ar-dating, palaeomagnetic, geochemical and mineralogical investigations. Austrian J Earth Sci 107:2–22

Rögl F (1994) *Globigerina ciperoensis* (Foraminiferida) in the Oligocene and Miocene of the Central Paratethys. Annalen des Naturhistorischen Museums in Wien Serie A für Mineralogie und Petrographie, Geologie und Paläontologie, Anthropologie und Prähistorie, pp 133–159

Rupp C, Haunold-Jenke Y (2003) Untermiozäne Foraminiferenfaunen aus dem oberösterreichischen Zentralraum. Jb Geol B-A 143:227–302

Rupp C et al (2008) Geologische Karte der Republik Österreich 1:50.000, Blatt 47 Ried im Innkreis. Erläuterungen zu Blatt 47 Ried im Innkreis. Geological Survey of Austria, Vienna

Sant K, Kirscher U, Reichenbacher B, Pippèrr M, Jung D, Doppler G, Krijgsman W (2017) Late Burdigalian sea retreat from the North Alpine Foreland Basin: new magnetostratigraphic age constraints. Global Planet Change 152:38–50. https://doi.org/10.1016/j.gloplacha.2017.02.002

Schlickum WR (1964) Die Molluskenfauna der Süßbrackwassermolasse Niederbayerns. Archiv für Molluskenkunde 93:1–70

Schlickum WR (1971) Die beiden miozänen Brackwasserbecken der süddeutschen Molasse und ihre Molluskenfauna. Senckenb Lethaea 52:569–581

Schlickum WR, Strauch F (1968) Der Aussüßungs- und Verlandungsprozeß im Bereich der Brackwassermolasse Niederbayerns. Mitteilungen der Bayerischen Staatssammlung für Paläontologie und Historische Geologie 8:327–391

Schlunegger F, Matter A, Burbank DW, Klaper EM (1997) Magnetostratigraphic constraints on relationships between evolution of the central Swiss Molasse basin and Alpine orogenic events. Geol Soc Am Bull 109:225–241. https://doi.org/10.1130/0016-7606(1997)109%3c0225:mcorbe%3e2.3.co;2

Schlunegger F, Melzer J, Tucker GE (2001) Climate, exposed source-rock lithologies, crustal uplift and surface erosion: a theoretical analysis calibrated with data from the Alps/North Alpine Foreland Basin system. Int J Earth Sci 90:484–499

Schneider S (2008) The bivalve fauna from the Ortenburg Marine Sands in the well-core "Straß" (Early Miocene; SE Germany)—taxonomy, stratigraphy, paleoecology, and paleogeography. Paläontol Z 82:402–417

Schneider S, Pippèrr M, Frieling D, Reichenbacher B (2011) Sedimentary facies and paleontology of the Ottnangian Upper Marine Molasse and Upper Brackish Water Molasse of eastern Bavaria: A field trip guide. In: GSA FIELD GUIDE. Geological Field Trips in Central Western Europe, vol 22. The Geological Society of America, pp 35–50. https://doi.org/10.1130/2011.0022(04)

Sissingh W (2006) Kinematic sequence stratigraphy of the European Cenozoic Rift System and Alpine Foreland Basin: correlation with Mediterranean and Atlantic plate-boundary events. Netherl J Geosci/Geologie en Mijnbouw 85:77–129

Spezzaferri S, Coxall HK, Olsson RK, Hemleben C (2018) Taxonomy, biostratigraphy, and phylogeny of Oligocene *Globigerina*, *Globigerinella*, and *Quiltyella* n. gen. In: Wade B, K. Olsson R, Pearson P, Huber B, Berggren W (eds) Atlas of Oligocene Planktonic Foraminifera, vol 46. Cushman Foundation for Foraminiferal Research, Lawrence, pp 179–215

ter Borgh M, Stoica M, Donselaar ME, Matenco L, Krijgsman W (2014) Miocene connectivity between the Central and Eastern Paratethys: constraints from the western Dacian Basin. Palaeogeogr Palaeoclimatol Palaeoecol 412:45–67. https://doi.org/10.1016/j.palaeo.2014.07.016

Teschner C, Reichenbacher B (2017) Otolith-based age determination of mid-Burdigalian marine sediments in the North Alpine Foreland Basin. Bull Geosci 92:143–152. https://doi.org/10.3140/bull.geosci.1659

Tipper JC, Sach VJ, Heizmann EPJ (2003) Loading fractures and Liesegang laminae: new sedimentary structures found in the north-western North Alpine Foreland Basin (Oligocene-Miocene, south-west Germany). Sedimentology 50:791–813. https://doi.org/10.1046/j.1365-3091.2003.00578.x

Unger HJ (1982) Die Forschungsbohrungen Osterhofen GLA 1—5, die Stratigraphie des tieferen Untergrundes und die Lagerung des Ortenburger Schotters. Verh Geol B-A 3:285–311

Unger HJ (1984) Geologische Karte von Bayern 1:50000—Erläuterungen zum Blatt Nr. L 7544 Griesbach im Rottal. Geologisches Landesamt für Umwelt, Munich

Unger HJ, Schwarzmeier J (1982) Die Tektonik im tieferen Untergrund Ostniederbayerns. Jahresbericht Oberösterreichischer Musealverein—Gesellschaft für Landeskunde 127:197–220

Van der Boon A et al (2018) The Eocene-Oligocene transition in the North Alpine Foreland Basin and subsequent closure of a Paratethys gateway. Global Planet Change 162:101–119. https://doi.org/10.1016/j.gloplacha.2017.12.009

von Hartmann H, Tanner DC, Schumacher S (2016) Initiation and development of normal faults within the German alpine foreland basin: the inconspicuous role of basement structures. Tectonics 35:1560–1574

Wagner LR (1998) Tectono-stratigraphy and hydrocarbons in the Molasse Foredeep of Salzburg, Upper and Lower Austria. Geol Soc Lond Spec Publ 134:339–369. https://doi.org/10.1144/GSL.SP.1998.134.01.16

Wenger WF (1987) Die Foraminiferen des Miozäns der bayerischen Molasse und ihre stratigraphische sowie paläogeographische Auswertung. Zitteliana 16:173–340

Wenger WF (1993) Biostratigraphische Untersuchungen in der Oberen Meeresmolasse bei Bad Füssing (Niederbayern)—Ein Beispiel für die praktische Anwendung mikropaläontologischer Untersuchungsmethoden bei der Standortoptimierung von Grundwassererschließungen. Zitteliana 20:411–417

Witt W (2000) Süßwasserostracoden der miozänen Vorlandmolasse Süddeutschlands. Mitteilungen der Bayerischen Staatssammlung für Paläontologie und Historische Geologie 40:109–151

Witt W (2009) Zur Ostracodenfauna des Ottnangs (Unteres Miozän) der Oberen Meeresmolasse Bayerns. Zitteliana 48(49):49–67

Zijderveld JDA (1967) A.C. demagnetization of rocks: analysis of results. In: Collinson DW (ed) Methods in Palaeo-magnetism. Elsevier, Amsterdam, pp 254–286